

## ACT LAUNCH Project No 299662



The LAUNCH project is funded through the ACT programme (Accelerating CCS Technologies, Horizon2020 Project No 294766). Financial contributions are made from: Netherlands Enterprise Agency (RVO), Netherlands; Bundesministerium für Wirtschaft und Energie (BMWi), Germany; Gassnova SF (GN), Norway; Department for Business, Energy & Industrial Strategy (BEIS) together with extra funding from NERC and EPSRC research councils, United Kingdom; US-Department of Energy (US-DOE), USA.  
All funders are gratefully acknowledged.



**Lowering Absorption process **UN**certainty, risks and **C**osts by predicting and controlling amine degradation**

### **Deliverable Nr. D1.3.1 and D4.2.1**

**Assessing the representativeness of accelerated degradation tests using the LAUNCH rigs and the DNM**

Dissemination level	Public	
Written By	E. Skylogianni, Y. A. Rueda Gomez, J. Monteiro (TNO); M. Akram, M. Pourkashanian (UoS); S.J. Vevelstad, A. Grimstvedt (SINTEF)	Date: 2/5/2023
Checked by WP4 Leader	Jon Gibbins	Date: 25/5/2023
Approved by the coordinator	Peter van Os	Date: 25/5/2023
Issue date	25/5/2023	

## Executive summary

Understanding key factors that accelerate solvent degradation in post-combustion CO<sub>2</sub> capture and developing an accelerated degradation protocol is an important feature in lowering the cost of solvent qualification, as it will allow for degradation trends to be observed in shorter test periods (typically within one month). One of the objectives of the LAUNCH project is to develop and validate a methodology for accelerating degradation while still obtaining industrially representative results.

The LAUNCH rig#2 (25 kg CO<sub>2</sub>/day) and the TERC plant (previous PACT plant, 1000 kg CO<sub>2</sub>/day) were used to investigate the capability of the much smaller LAUNCH rig#2 to mimic the degradation trends of larger plants as well as study various strategies to accelerate degradation. Four accelerated degradation techniques were studied: increased oxygen levels in the flue gas, increased solvent concentration, increased stripping temperature, and addition of NO<sub>x</sub> to the flue gas. For the *Baseline* campaign, 7.6 vol% oxygen concentration was considered in the flue gas, since this is representative of industrial gases. The accelerated degradation techniques were applied in different operational campaigns:

Campaign name	Description
Baseline	34 wt% MEA, 7.6 vol% O <sub>2</sub> , 120 °C
Higher O <sub>2</sub> *	35 wt% MEA, 19.8 vol% O <sub>2</sub> , 120 °C
Higher O <sub>2</sub> /MEA	37 wt% MEA, 19.8 vol% O <sub>2</sub> , 120 °C
Higher O <sub>2</sub> /stripping T	35 wt% MEA, 19.8 vol% O <sub>2</sub> , 130 °C
Higher O <sub>2</sub> /NO <sub>x</sub>	35 wt% MEA, 19.5 vol% O <sub>2</sub> , 120 °C, NO <sub>x</sub>

\* reported in D4.1.1

The major degradation products were HEPO, MEA-Urea and HEGly, while formic acid was the most dominant acid. Iron concentrations up to 4 mg/kg were seen in TERC and up to 7 mg/kg in the LAUNCH rig#2. In addition the concentration of zinc (Zn - a known degradation catalyst) in LAUNCH rig#2 was possibly significant, sometimes exceeding the Fe concentration; the source of it is suspected to be a heating element in the rig. Zinc and copper construction materials would not normally be expected to be included in the wetted path of amine capture plants. Although it is seen that the LAUNCH rig#2 is capable of predicting the degradation trends and the most significant degradation products as larger rigs, such as TERC, it is noted that when comparing the trends between the two rigs, we see significant differences regarding the accelerated degradation strategy that yields higher degradation. For example, highest HEPO, MEA-Urea and Fe concentration were found at the *Higher O<sub>2</sub>/stripping T* campaign in the LAUNCH rig, while this was the case for *Higher O<sub>2</sub>/MEA* campaign at TERC. The campaigns were performed with the two rigs in similar, but not identical, conditions, therefore longer tests and more similar operating conditions can possibly explain the differences seen in the degradation trends.

Overall, increasing the oxygen content in the flue gas from 7 vol% to 18 vol% clearly accelerates degradation. The *Baseline* campaign with 7 vol% O<sub>2</sub> shows lower concentration for both degradation products and metals when compared to the *Increased O<sub>2</sub>* campaign. Although the *Increased O<sub>2</sub>* campaign in the LAUNCH rig#2 had a higher Fe starting concentration, which is expected to have also contributed to the degradation progression in the solvent, it is seen that the *Baseline* campaign has the lowest degradation products concentration of all the campaigns, demonstrating that *Increasing O<sub>2</sub>* content in the flue gas is a successful technique for accelerating degradation. In the TERC campaigns, the *Baseline* campaign shows also the lowest concentration of organic degradation compounds, and specifically the most dominant ones HEPO and MEA-Urea. However, the *Higher O<sub>2</sub>/MEA* and *Higher O<sub>2</sub>/stripping T* campaigns had lower formic acid concentration than the *Baseline*, the reason for which is not clear.

Increasing the MEA content of the solvent does not seem to have a strong influence on the acceleration of the oxidative degradation products (acids), although it has an increasing effect on the metal accumulation seen in the studied systems. The *Higher O<sub>2</sub>/MEA* campaign yields the highest concentration of HEPO and MEA-Urea, according to the results from TERC. In the LAUNCH rig#2, such trend is not shown, however the reason for this might be the lower MEA concentration (~37 wt% MEA) compared to TERC (~40 wt% MEA), as a result of water imbalance in the system and thus difficulty to control the solvent composition. Regarding metals, in TERC, the iron content is higher than in the rest of the campaigns, though it is noted that the iron

method used in this work is a colorimetric method, which is more prone to higher uncertainties due to the potential connection of the solvent color with degradation. In the LAUNCH rig#2, the iron content is generally higher in the *Higher O<sub>2</sub>/MEA* campaign, though it is exceeded towards the end of the campaigns in the case of *Higher O<sub>2</sub>/stripping T*.

Increasing the stripping temperature does not seem to affect the formation of oxidative degradation products, meaning formic and oxalic acid, while it led to the highest concentrations of HEPO and MEA-Urea and metal accumulation in the system compared to the rest of the campaigns. These trends are demonstrated with the LAUNCH rig#2. A comparison and drawing conclusions based on the TERC results is more challenging due to the facts that the temperature was increased to 128 °C in TERC (instead of 130 °C) and, mainly, because the stripping pressure remained the same, thus leading to lower loadings than in the rest of the campaigns, making the comparison invalid (although the use of higher reboiler temperatures to obtain lower lean loadings is a likely operational combination in industrial practice (Michailos, 2022) and lower lean loadings were also predicted to reduce thermal degradation in work for LAUNCH WP1 (Mullen, 2023)).

The effectivity of adding NO<sub>x</sub> in the flue gas as an accelerating degradation technique is shown to be dependent on the level of NO<sub>x</sub> added and the degradation product targeted. Tests in the LAUNCH rig#2 with 169 ppmv show a sharp increase in the formation of acids, specifically formic acid, while the HEPO and MEA-Urea concentration were at the same level as the *Increased O<sub>2</sub>* campaign. Metals also remained at the same level as the *Baseline*. Tests in TERC were conducted with 15 ppmv, which is much lower than in the LAUNCH rig#2 and more representative of industrial flue gases. The campaign with *Increased O<sub>2</sub>/NO<sub>x</sub>* showed higher formic acid concentration than the other campaigns, but no higher than the *Increased O<sub>2</sub>* one. No clear effect is shown when comparing HEPO and MEA-Urea products, since HEPO concentration by the end of the campaign is similar to the *Increasing O<sub>2</sub>/MEA* campaign, which yielded the higher concentration, while MEA-Urea concentration is lower than the *Baseline* campaign. The metal concentration was similar to the *Baseline* campaign, in agreement with LAUNCH rig#2 findings.

Altogether, the LAUNCH rig was found capable of predicting the major degradation components found in the larger TERC pilot plant. The above-mentioned differences in the degradation trends are believed to be the result of running at similar, but not identical, conditions and parameters in the two plants, as a result of either operational challenges or system/measuring method limitations.

Moreover, within LAUNCH, a predictive tool for amine degradation was developed, called Degradation Network Model (DNM), which is presented in report *D1.3.4 Degradation Network model*. In this work, the DNM model predictions were compared with the experimental results of two campaigns; one with ~37 wt% MEA and 19.8 vol% O<sub>2</sub>, and one with ~34 wt% MEA and 7.6 vol% O<sub>2</sub> in the flue gas (dry basis). It was found that the model captures the general trend of the results, by predicting that the degradation for the higher oxygen campaign is higher than in the lower oxygen campaign, which is also seen in the experimental results. The model consistently underpredicts the degree of oxidative degradation for both campaigns, while for each campaign, the level of relative deviation (RD) remains approximately the same along the campaign. In the high oxygen campaign, the relative deviation between the predicted and measured values is -76% and, in the lower oxygen campaign, it is -30%. Hence, the model yields better results for the lower oxygen case. This points towards the fact that the model is developed and "calibrated" with degradation data from real operation of a CO<sub>2</sub> capture pilot plant with specific oxygen content in the flue gas, as well as using 30 wt% MEA. Other sources of error are the high uncertainty in ammonia measurement, presence of additional oxidative and thermal degradation products as well as metals which are not accounted in the model.



## Table of Contents

<b>1</b>	<b>INTRODUCTION</b>	<b>5</b>
<b>2</b>	<b>DEGRADATION CAMPAIGN WITH LAUNCH RIG#2</b>	<b>6</b>
2.1	DESCRIPTION OF LAUNCH RIG#2	6
2.2	ACCELERATED DEGRADATION TESTS IN LAUNCH RIG#2	7
2.2.1	<i>Operation</i>	7
2.2.2	<i>Analytical measurements</i>	9
<b>3</b>	<b>DEGRADATION CAMPAIGNS IN TERC</b>	<b>13</b>
3.1	DESCRIPTION OF TERC	13
3.2	ACCELERATED DEGRADATION TESTS IN TERC	15
3.2.1	<i>Operation</i>	15
3.2.2	<i>Analytical measurements</i>	17
<b>4</b>	<b>MAIN FINDINGS FROM THE LAUNCH RIGS' CAMPAIGNS</b>	<b>21</b>
<b>5</b>	<b>EVALUATION OF RESULT USING THE DNM MODEL</b>	<b>23</b>
<b>6</b>	<b>CONCLUSIONS</b>	<b>25</b>
<b>7</b>	<b>REFERENCES</b>	<b>27</b>
	<b>APPENDICES</b>	<b>28</b>
	<b>APPENDIX A. OVERVIEW OF COMPONENTS AND ANALYTICAL METHODS</b>	<b>28</b>
	<b>APPENDIX B. TROUBLESHOOTING</b>	ERROR! BOOKMARK NOT DEFINED.
	<b>APPENDIX C. ANALYTICAL MEASUREMENTS</b>	<b>31</b>

## 1 Introduction

Understanding key factors to accelerate solvent degradation in post-combustion CO<sub>2</sub> capture plants and developing an accelerated degradation protocol is an important feature in lowering the cost of solvent qualification, as it will allow for degradation trends to be observed in shorter test periods (typically one month). The overall objective is to develop a methodology for accelerating degradation while still obtaining industrially representative results.

The LAUNCH rig#2 and the TERC plant (previous PACT plant) were used in order to develop various strategies to accelerate degradation and gain input for the design of the protocol.

Four accelerated degradation techniques have been identified and studied: increased oxygen levels in the flue gas, increased solvent concentration, increased stripping temperature, and addition of NO<sub>x</sub>. Oxygen is known to be a key cause of (oxidative) degradation, therefore higher degradation rates are expected at the presence of higher oxygen content. Concentrated MEA (cMEA) is a second-generation solvent being proposed for commercial use (Reddy & Gilmatrin, 2008) and refers to concentrations higher than and including 35 wt%. Based on limited public domain experience, while higher MEA concentrations give improved energy consumption and reaction rates, they also can exhibit higher rates of degradation (Morken et al., 2019). As far as higher stripping temperature is concerned, it is evident that at higher temperatures, the rate of the degradation reactions, both related to thermal and oxidative degradation, will be accelerated. Finally, the presence of nitrogen oxides has been shown to contribute to oxidative degradation of the solvent, as it results in reactive species (Fine Nathan, 2015).

A series of campaigns using these techniques and their combinations were designed and performed. The different acceleration techniques were examined with a total test time of more than 750 hours, with a minimum duration of 150 hours for each test. Campaigns were conducted using 7 and 18 vol% oxygen in the flue gas, the MEA concentration increased from 35 to 38 wt%, the reboiler temperature 120 to 130 °C and up to 300 ppmv NO<sub>x</sub> were added in the study of the last accelerated degradation strategy. An overview of the campaigns performed is given in sub-section 2.2, Table 1.

The tests were designed to be undertaken first in LAUNCH Rig#2 operated by TNO and, afterwards, in the TERC pilot rig by the University of Sheffield. However, it is noted that the campaigns were performed with the two rigs in similar, but not identical, conditions, therefore some differences in the trends were expected. SINTEF IND contributed with sample analysis and advise on trends obtained in LAUNCH rig#1, in previous projects. After each test the degraded solvent was removed, and fresh solvent was used. This was decided in an effort to have the same starting point when comparing the different accelerated degradation techniques and, therefore, being able to make clear distinct conclusions.

In sections 2 and 3, the results from LAUNCH rig#2 and TERC, respectively, are reported in terms of operational parameters and analytical measurements, after first giving an overview of the campaigns performed. Section 4 includes the assessment of the representativeness of accelerated degradation tests using the LAUNCH rigs of both the LAUNCH rig#2 and the TERC, while in Section 5 an evaluation is performed using the Degradation Network Model (DNM). Section 6 concludes the work and proposes future work.

## 2 Degradation campaign with LAUNCH rig#2

### 2.1 Description of LAUNCH rig#2

TNO's LAUNCH rig#2 is a CO<sub>2</sub> capture plant (5 Nm<sup>3</sup>/h flue gas capacity) which allows for 24/7 continuous operation of the system. It enables tests of different solvents, multiple technologies for solvent management (oxygen removal, iron removal) and process quality control under realistic conditions at TRL5. The rig can be operated with artificial or real flue gas; however, this campaign was done with artificial flue gas in a composition similar to the ones of gas turbines. The gas inlet is controlled by mass flow controllers and an evaporator is connected to the lines to guarantee that the flue gas is saturated with water prior to entering the absorber column.

The gas outlet of the absorber column is connected to a flow meter and a Fourier-transform Infrared Spectrometer (FTIR) to allow for quantification of emissions and enable the calculation of capture rate. On the stripper side, an electrical heater is used in the reboiler and the gas outlet is monitored with the use of a mass flow meter. Similar to the work in Task 4.1, during the accelerated degradation tests in Task 4.2, the rig was not equipped with water washes. Figure 1 illustrates LAUNCH rig#2 at TNO.



Figure 1: LAUNCH rig#2 at TNO

## 2.2 Accelerated degradation tests in LAUNCH rig#2

Five campaigns were performed in order to study the factors leading to accelerated degradation and the extend at which the degradation is accelerated. An overview is shown in Table 1, followed by two sub-sections: one concerning the operation and one concerning the analytical.

**Table 1 – Overview of campaigns for accelerated degradation investigations. CO<sub>2</sub> content is 5.5 vol% (dry) and oxygen content is given in dry basis**

Campaign #	Description	Duration (h)	Name	Comment
2*	37 wt% MEA, 19.8 vol% O <sub>2</sub> , 120 °C	384	Higher O <sub>2</sub> /MEA	
3	35 wt% MEA, 19.8 vol% O <sub>2</sub> , 130 °C	360	Higher O <sub>2</sub> /stripping T	
4**	35 wt% MEA, 19.8 vol% O <sub>2</sub> , 120 °C, NO <sub>x</sub>	240	-	NO <sub>x</sub> : 144 ppmv
5	34 wt% MEA, 7.6 vol% O <sub>2</sub> , 120 °C	360	Baseline	
6	35 wt% MEA, 19.5 vol% O <sub>2</sub> , 120 °C, NO <sub>x</sub>	240	Higher O <sub>2</sub> /NO <sub>x</sub>	NO <sub>x</sub> : 169 ppmv

\*Starting from 2, assuming that the long campaign described in D4.1.1. is Campaign 1, named "Higher O<sub>2</sub>".

\*\*Results not reported further in the report due to unstable operation and mist formation

One might notice that in Campaign 5, where the effect of oxygen concentration is studied, it was decided to decrease the oxygen content. The decision was made upon agreement with the TERC team due to HSE concerns regarding operation of the rigs at oxygen concentrations higher than 20 vol%, thus, approaching the components' explosive limits. This campaign is the baseline with lower O<sub>2</sub> concentration, which is also representative for industrial flue gases. In addition, both campaigns #4 and #6 were conducted in the presence of NO<sub>x</sub>. The reason for this is that in Campaign #4, the NO<sub>x</sub> control was challenging, and severe mist was formed in the outlet of the absorber, while in Campaign #6 these issues were fixed by adding a filter before the absorber. The results from Campaign #4, thus, are not included in the analytical results.

### 2.2.1 Operation

Before any new campaign was started, the LAUNCH rig#2 was washed with water and emptied using compressed air. Fresh MEA was prepared and added in the rig. The main operational information, such as flows, temperatures, pressures, are presented for each campaign in Table 2.

**Table 2: LAUNCH rig#2 operation parameters (mean values)**

Parameter	Unit	Campaign #2	Campaign #3	Campaign #4	Campaign #5	Campaign #6
<b>Absorber</b>						
Temperature Gas inlet	°C	37.5	37.2	37.5	36.1	36.6
Pressure Gas inlet	mbarg	50.40	48.70	36.20	40.30	38.90
Air inlet flowrate	nL/h	4225	4134	3779	1600	3298
O <sub>2</sub> inlet flowrate	nL/h	887	868	794	336	693
CO <sub>2</sub> inlet flowrate	nL/h	246	245	230	243	245
Inlet flowrate dry total	nL/h	4471	4379	4009	4443	3543
H <sub>2</sub> O inlet flowrate	g/h	192	187	156	173	179
H <sub>2</sub> O inlet flowrate	nL/h	239	233	195	216	224
Inlet NO concentration	mg/Nm <sup>3</sup>	-	-	135	-	170
Inlet NO <sub>2</sub> concentration	mg/Nm <sup>3</sup>	-	-	89	-	86
Inlet flowrate wet total	nL/h	4710	4612	4204	4660	3767
Gas inlet composition, CO <sub>2</sub>	vol(%) dry	5.49	5.60	5.74	5.5	6.9
Gas inlet composition, CO <sub>2</sub>	vol(%) wet	5.21	5.32	5.47	5.2	6.5
Gas inlet composition, O <sub>2</sub>	vol(%) dry	19.8	19.8	19.8	7.6	19.5



Gas inlet composition, O <sub>2</sub>	vol(%) wet	18.8	18.8	18.9	7.2	18.4
Gas inlet composition, H <sub>2</sub> O	vol(%)	5.1	5.1	4.6	4.6	5.9
Lean solvent inlet temperature	°C	39.7	40.0	39.8	39.9	40.0
Lean solvent inlet pressure	mbarg	526	522	520	512	514
Lean solvent inlet flowrate	kg/h	11.4	11.5	11.5	11.2	11.5
Lean solvent density	kg/m <sup>3</sup>	1091	1095	1109	1089	1095
Lean solvent outlet flowrate	m <sup>3</sup> /h	0.010	0.010	0.010	0.010	0.010
Rich solvent outlet temperature	°C	39.2	39.6	37.9	38.5	39.4
Rich solvent outlet pressure	mbarg	1195	1868	1096	1104	1072
Rich solvent outlet flowrate	kg/h	12.0	12.1	12.1	11.9	12.2
Rich solvent density	kg/m <sup>3</sup>	1119.0	1113.8	1120.0	1110.0	1113.0
Rich solvent outlet flowrate	m <sup>3</sup> /h	0.011	0.011	0.011	0.011	0.011
abs T profile (top)	°C	56.60	55.90	52.40	55.90	55.80
abs T profile	°C	61.20	60.20	56.80	60.30	60.40
abs T profile	°C	59.70	58.50	55.00	58.7	59.00
abs T profile	°C	55.6	54.8	51	54.4	55.2
abs T profile (bottom)	°C	48.3	48	44.8	47.1	48.2
Liquid volume absorber sump	m <sup>3</sup>	0.0012	0.0007	0.0008	0.0013	0.0022
Residence time absorber sump	min	6.7	4.1	4.3	7.2	12.1
Gas outlet temperature	°C	39.1	36.4	34.5	36.7	37.1
Pressure outlet	mbarg	23.5	21.3	12.9	15.1	13.8
CO <sub>2</sub> outlet to vent*	vol(%) wet	0.56	0.65	2.27	0.43	1.35
H <sub>2</sub> O outlet to vent*	vol(%)	7.04	6.07	5.47	6.17	6.31
MEA outlet to vent*	mg/Nm <sup>3</sup>	97.3	23.4	147.6	1.5	308.1
NH <sub>3</sub> outlet to vent*	mg/Nm <sup>3</sup>	12.4	10.4	10.3	3.4	7.7
NO outlet to vent	mg/Nm <sup>3</sup>	-	-	111	-	136
NO <sub>2</sub> outlet to vent	mg/Nm <sup>3</sup>	-	-	57	-	59
<b>Stripper</b>						
Rich solvent inlet temperature	°C	90.9	107.0	101.0	96.3	104.0
Rich solvent inlet pressure	mbarg	1090	1739	932	963	897
Gas outlet to condenser	°C	86.3	101.0	95.3	93.3	101.0
Pressure outlet to condenser	mbarg	809.70	590.00	788.00	756.00	760.20
Lean solvent outlet pressure	mbarg	659	1420	646	617	608
stripper T profile (top)	°C	91.9	107.0	101.0	98.0	105.0
stripper T profile	°C	92.9	108.0	101.0	99.2	106.0
stripper T profile	°C	93.8	107.0	101.0	100.0	107.0
stripper T profile	°C	101.0	110.0	103.0	106.0	110.0
stripper T profile (bottom)	°C	113.0	121.0	112.0	115.0	115.0
Reboiler duty	kW	0.87	1.01	0.9	0.98	1.13
Liquid volume in reboiler	m <sup>3</sup>	0.006	0.006	0.006	0.006	0.006
Residence time in reboiler	min	34.2	33.8	33.9	36.2	34.8
Temperature in reboiler liquid	°C	120.1	130.1	120.1	120.0	120.0
Temp CO <sub>2</sub> product from condenser	°C	15.5	18.0	18.8	18.2	19.6
Flow CO <sub>2</sub> product from condenser	L/h	228.68	209.35	187.13	205.83	197.90
	nL/h	216.40	196.41	175.08	192.97	184.65
<b>Cross heat exchanger</b>						
Cold rich inlet temperature	°C	38.3	38.7	37.1	37.7	38.6
Cold lean outlet temperature	°C	41.0	42.2	40.8	40.8	42.1
Hot rich outlet temperature	°C	98.2	112.3	106.1	103.5	108.5

Hot lean inlet temperature	°C	113.4	125.1	115.4	115.4	116.8
Residence time in rich hot line (cross heat exchanger to stripper)	min	1.3	1.3	1.3	1.4	1.3

\*corrected values due to FTIR leakage, thus higher uncertainty.

Similar to the longer campaign in Task 4.1, the campaigns were overall stable, with the exception of Campaign #4. The reason was severe mist formation (**Error! Reference source not found.**), therefore the campaign was repeated as Campaign #6. In Campaign #6, pure NO was used which together with the air in the gas led to NO<sub>x</sub> concentration in the inlet of 169 ppmv (256 mg/Nm<sup>3</sup>), from which 127 ppmv NO<sub>2</sub> and 42 ppmv NO.

The lean and rich loadings are reported as the average value along each campaign and the reported values are measured by FTIR (liquid samples). The data processing follows the approach followed in Task 4.1., where density values are calculated according to the model proposed by Han et al. (Han et al., 2012). Furthermore, the capture rate is calculated both by using the measurements in the gas side and the measurements in the liquid side. An overview of the achieved loadings, cyclic capacity and capture rates in each campaign is presented in Table 3. The corresponding values from the long campaign (Campaign #1) are also listed for comparison purposes.

**Table 3: Overview of loadings, cyclic capacity and capture rates in LAUNCH rig#2**

Campaign	Lean loading (mean)	Rich loading (mean)	Cyclic capacity	Capture rate (gas side)	Capture rate (liquid side)
	mol CO <sub>2</sub> /mol MEA			%	
1	0.27	0.44	0.17	87	88
2	0.28	0.44	0.16	88	95
3	0.30	0.45	0.15	81	80
4	0.38	0.46	0.12	77	74
5	0.28	0.45	0.16	80	88
6	0.27	0.42	0.15	76	89

The capture rates calculated with two different ways are generally in a good agreement, except for Campaign #2 and Campaign #6 which show a higher difference. This can be the result of uncertainty in the mass flow controllers, in the CO<sub>2</sub> flow measurement as well as in the loading determination.

With the help of the FTIR on the top of the absorber, the MEA and ammonia emissions were followed (see Table 2). In average, the campaigns in the presence of high levels of NO<sub>x</sub> had the higher MEA emissions (150-300 mg/Nm<sup>3</sup>). The lowest emissions were recorded during the campaign with decreased oxygen concentration (Campaign #5) where the average value for MEA was 2 mg/Nm<sup>3</sup> and for ammonia 3 mg/Nm<sup>3</sup>. Both the MEA and the ammonia emissions in the longer campaign were higher than in the campaigns #2 to #6.

### 2.2.2 Analytical measurements

Various analytical methods have been used. These are explained in D.4.1.1, therefore they are not further elaborated here but rather a list of components and respective analysis method is given in the Appendix. It is noted that the analysis for the acids was performed in TNO's analytical laboratory for the LAUNCH rig#2, while for TERC, they were analysed by SINTEF. For the data processing details, the reader is directed to D4.1.1 as well.

As mentioned earlier, the LAUNCH rig#2 was washed with water and emptied using compressed air after every campaign, followed by filling with fresh MEA solvent. Due to the fact that some water might be left from the washing in the cross-heat exchanger, the starting concentration reported in this report is the one after filling the plant (measured by FTIR), and not the one based on the gravimetric data. Moreover, as mentioned earlier, Campaign #4 was not stable due to mist formation and, thus, lasted for a short period of time. For this reason, the analytical results from Campaign #4 are not shown in the results below.

During the campaigns, MEA concentration was shown to decreasing, which can also indicate degradation of MEA. From the components analyzed, acetic acid, HEEDA, 2-oxazoline and lead were not detected. For all analyzed compounds, the campaign with the lower O<sub>2</sub> content (*Baseline*) showed the lowest concentration from the other campaigns. This includes also ammonia, as measured in the gas phase in the outlet of the absorber.

Formic acid and oxalic acid were formed and increased along the campaigns, with formic acid detected at higher concentration than oxalic acid (formic acid formation trends shown in Figure 2). A sharp increase is shown in the presence of NO<sub>x</sub>, as well as in the *Higher O<sub>2</sub>* campaign. As explained later in the discussion about the metal content, the *Higher O<sub>2</sub>* campaign had an iron concentration of 5 mg/kg already from the start of the campaign, that can be playing an accelerating role in the formation of the degradation products. An apparent shift on behavior is depicted in the last point of the *High T* campaign,

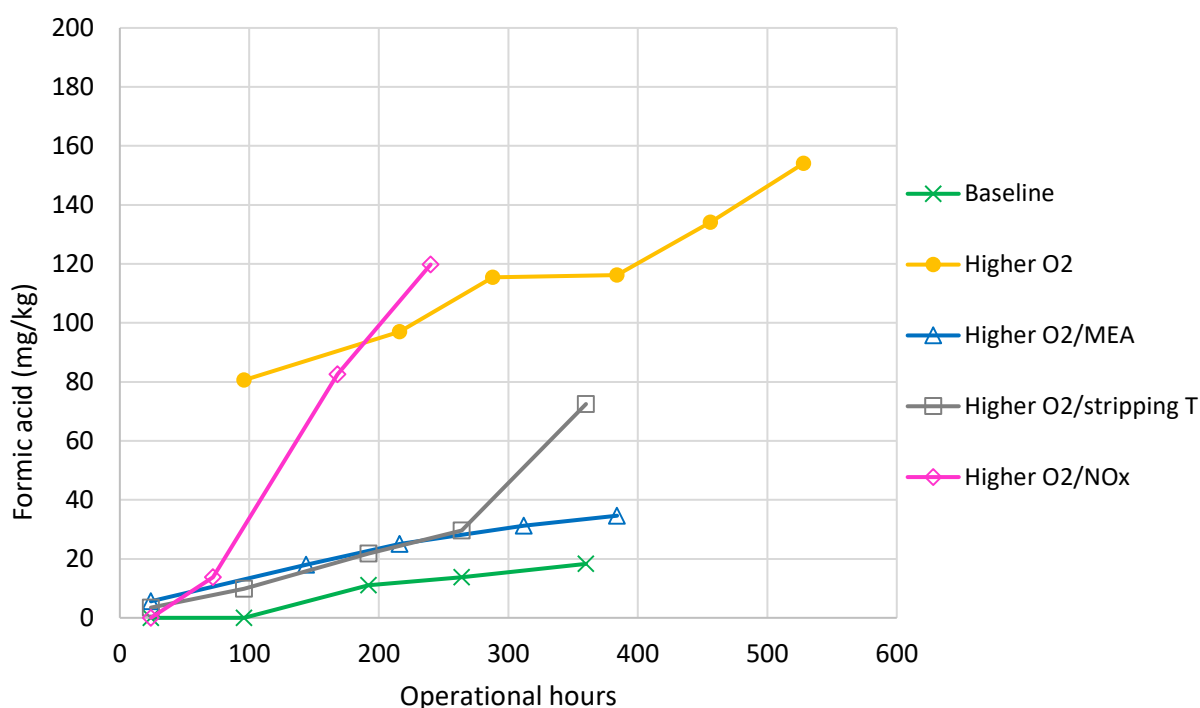


**Figure 2: Formic acid expressed in CO<sub>2</sub>-free basis and water-corrected during the accelerated degradation campaigns in the LAUNCH rig#2**

As far as the organic compounds measured by LC-MS are concerned, it is seen that their concentration remains relatively constant throughout the campaign with the exception of HEPO and MEA-Urea. HEPO concentration increases sharply, while the slope of the MEA-Urea is lower. In Figure 3, one can see the progress of the concentration of these two major degradation components. The highest concentration of HEPO and MEA-Urea is seen in the campaign with increased reboiler temperature, and the lowest concentration is seen in the campaign with decreased oxygen content. HeGly and HEF are also identified as major components, following HEPO and MEA-Urea, in different degree and order in the different campaigns. Furthermore, the shift of the overall behavior in the last point of the *High O<sub>2</sub>/stripping T* campaign that was observed in Figure 2, is seen also for HEPO, however not for MEA-Urea. Therefore, this point is not considered an outlier, but rather indicates interplays among the degradation compounds at those conditions (no operational changes occurred that could explain this change in degradation behavior).

Various metals were also analysed since not only can they give insights regarding the corrosivity of the system, but also because literature on solvent management generally agrees that the metals' content in the solvent is a key determinant aspect of the degradation rate (Chi & Rochelle, 2002; Léonard et al., 2014). The

concentration trends were similar from one campaign to the other, therefore the concentration of all metals is shown only for one campaign (*Higher O<sub>2</sub>/stripping T*, Figure 4). It is seen that iron and zinc (a known MEA degradation catalyst) concentration are higher than the rest of the metals, whose concentrations do not exceed 2 mg/kg. In the *Baseline* campaign and the *Higher O<sub>2</sub>/NO<sub>x</sub>* campaign, these concentrations were lower with maximum value of 2 mg/kg. Moreover, in these two campaigns, the Zn concentration exceeded the Fe concentration and the source of it is suspected to be a heat element in the rig. This happened after 15 days in the low oxygen campaign, but only after 7 days in the *Higher O<sub>2</sub>/NO<sub>x</sub>* campaign. It is noted that the NO<sub>x</sub> campaign (#6) lasted less than the other campaigns, due to the troubleshooting efforts in Campaign #4.

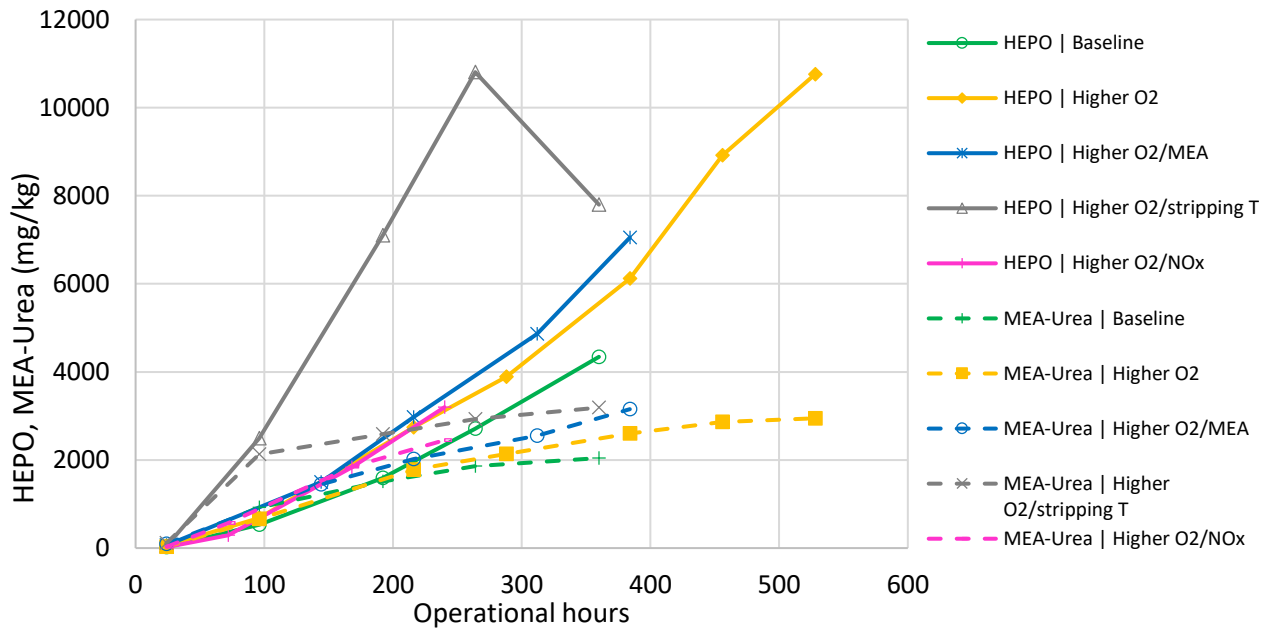


**Figure 3: HEPO (continuous lines) and MEA-Urea (dashed lines) concentration expressed in CO<sub>2</sub>-free basis and water-corrected during the accelerated degradation campaigns in the LAUNCH rig#2**

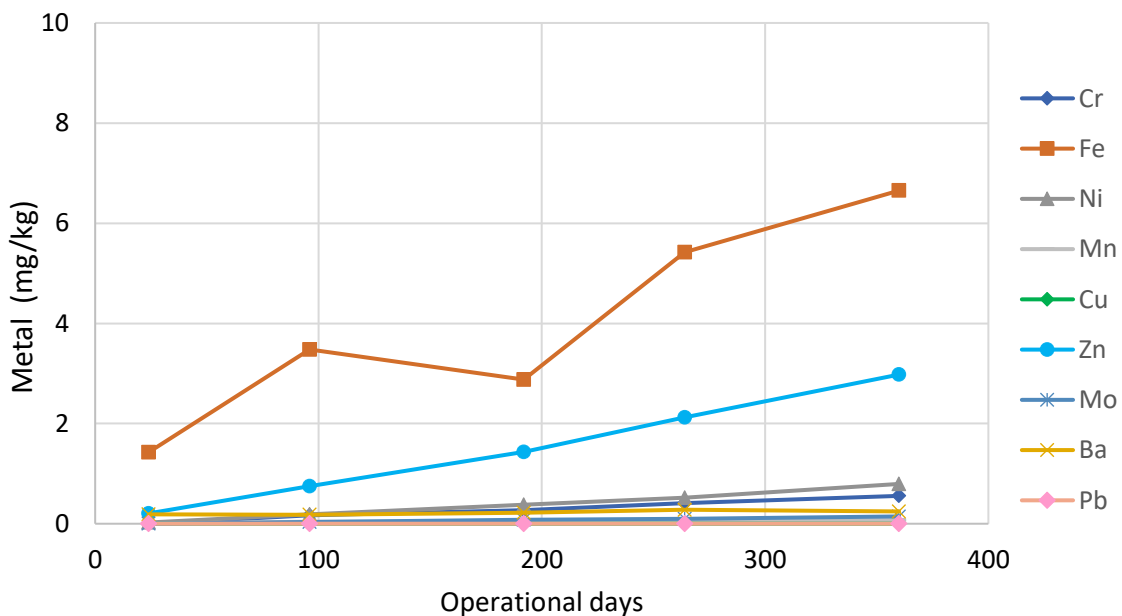


**Figure 4: Metals' concentration expressed in CO<sub>2</sub>-free basis and water-corrected along the increased reboiler temperature campaign ("Higher stripping T") in the LAUNCH rig#2**

In addition, the iron concentration has been plotted against time for all accelerated degradation campaigns in Figure 5. The highest formation rate is shown for the Higher stripping T campaign, with a clearly sharper slope compared to all other campaigns. The fact that the Fe amount starts higher in the Higher O<sub>2</sub> campaign than the rest of the campaigns is attributed in using bulk MEA which can carry metal traces from the transport container. Moreover, iron appears in higher concentrations in the Higher wt% MEA campaign, and lowest for the *Baseline* and *Higher O<sub>2</sub>/NOx* campaigns.

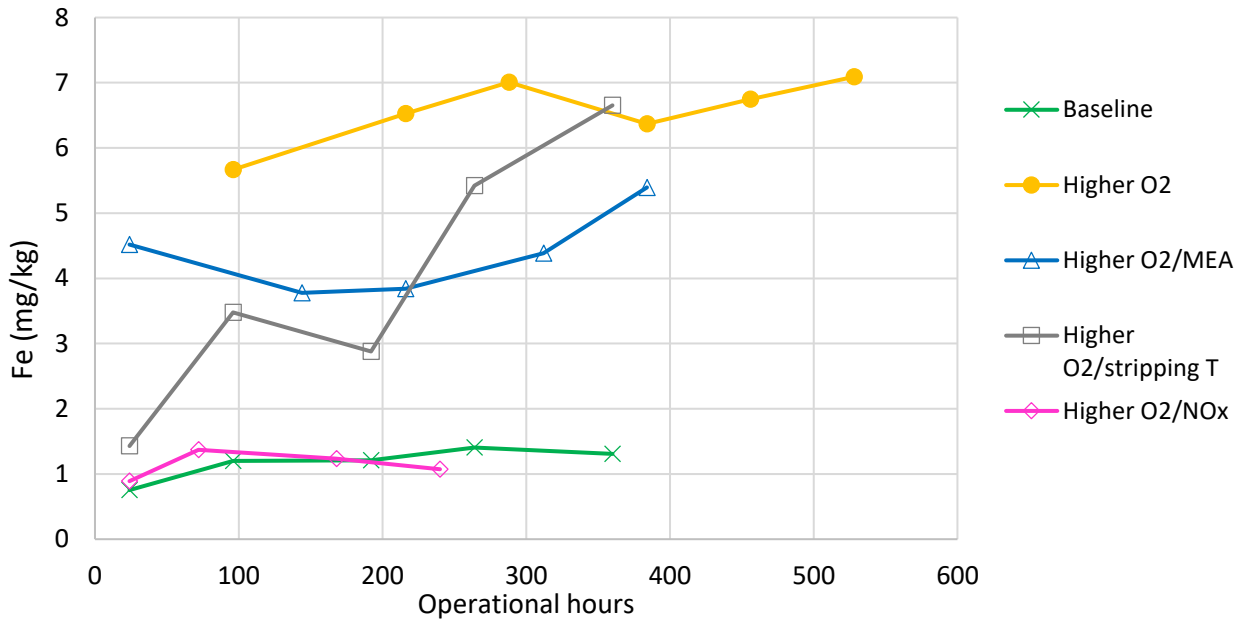


**Figure 5: Iron concentration expressed in CO<sub>2</sub>-free basis and water-corrected during the accelerated degradation campaigns in the LAUNCH rig#2**

## 3 Degradation campaigns in TERC

### 3.1 Description of TERC

The pilot scale CO<sub>2</sub> capture plant at TERC, shown in Figure 6, is capable of capturing 1tpd CO<sub>2</sub> based on 200 Nm<sup>3</sup>/h gas flow having 15% CO<sub>2</sub> i.e., the plant is designed for coal combustion flue gases. The plant is integrated with site combustion facilities including: Grate Boiler/Waste to Energy plant; Gasifier CHP; Biodiesel CHP, Gas Turbine CHP and a visiting/future rigs. It is designed to scrub 100-250 Nm<sup>3</sup>/h of flue/process gas with solvent flows of 300-1600 kg/h based on current packing. The plant can also be fed from a dedicated synthetic gas mixing skid comprising 3 bulk gas streams: CO<sub>2</sub>, N<sub>2</sub> and Air, each of 6-300Nm<sup>3</sup>/h flow range and a trace gas (NO<sub>2</sub>, SO<sub>2</sub>) injection capability; this enables the simulation or modulation of a range of combustion/process gases. Equipment specifications are given in Table 6. The plant has a full absorption and desorption cycle and is equipped with two absorber vessels that can be connected in series, a stripper, a reboiler, a cross exchanger, a carbon filter and a water wash. The plant also has a gas pre-treatment section which can be used either as a Flue Gas Desulphurisation (FGD) unit or a Direct Contact Cooler (DCC). The plant has recently been upgraded to including gas humidification control in the DCC. However, during these tests the FG/DCC was bypassed.



Figure 6: TERC CO<sub>2</sub> capture plant

Two absorber vessels are installed in series to increase residence time and contact between liquid and gas. Each of the absorbers is equipped with two beds of Flexipac 350X structured packing, 3m each. Total packed height, therefore, is 4 beds of 3 m each, so totalling 12 m, with liquid re-distribution at each bed. The stripper is packed with 7 m of IMTP25 random packing. The absorbers have 12 temperature measurement points each for temperature profiling.

Stripping is performed in the stripper and reboiler. The stripper is a 0.3 m diameter column packed with IMTP25 random packing. The reboiler is a shell and tube heat exchanger. Pressurized hot water (PHW) generated by electrical heating is supplied on the tube side of the reboiler while solvent stays on the shell side. The PHW has a bypass to control the flow rate through the reboiler or to bypass it. A pneumatically driven 3-way valve is used for this purpose. The energy used for stripping is calculated by measuring the inlet and outlet temperatures and the flow rate of the PHW. Stripper pressure is controlled automatically to a user defined set point.

The CO<sub>2</sub> product stream leaving the top of the stripper is passed through a condenser to remove steam and solvent vapours. The condensed liquid is separated from the gas in a reflux drum and is sent back to the stripper through a U-seal mechanism, while CO<sub>2</sub> is exhausted to atmosphere after analysis.

A blower is used to drive the gas through the plant. For this test campaign, air with CO<sub>2</sub> injection, rather than real flue gas, was used, to give enhanced O<sub>2</sub> levels. The tests were performed under general gas turbine conditions so the CO<sub>2</sub> concentration in the absorber entry gas was kept close to 5%.

CO<sub>2</sub> flow was measured by thermal mass flow meters, while the flow rate of gas into the absorber was measured by a pitot type flow meter. Gas composition for mass balance calculations was measured at the inlet and outlet of the absorber, along with temperature and pressure.

**Table 4: Absorber and stripper specifications**

Specifications	Absorber	Stripper	Water wash
Diameter (mm)	250	300	300
Packing name	Flexipak 350X	IMTP25	IMTP25
Packing type	Structured	Random	Random
Packing height (m)	12	7.5	7.5
Packed beds	4	1	1
Temperature measurements	24	9	-

Process and analytical measurements are described in Table 5. Gas analysis can be performed at 6 different locations in the plant. Sampling lines are located at the FGD inlet, Absorber 1 inlet, Absorber 2 inlet, Water wash inlet and outlet, and Stripper outlet.

**Table 5: Process and analytical measurements**

Analysis	Detail
Main Process parameters	<ul style="list-style-type: none"> <li>• Gas inlet flow, temperature and pressure</li> <li>• Interstage gas temperatures and pressures</li> <li>• Absorber 1 &amp;2 and desorbed temperature profiles and pressure drops</li> <li>• Desorber pressure (reflux condenser) and CO<sub>2</sub> product flow</li> <li>• Liquid flows, temperatures pressures and densities</li> <li>• Reboiler hot water flow; inlet, outlet, core temperature; supply pressure</li> </ul>
Gas analysis	Multipoint sampling and analysis by GasMET FTIR: <ol style="list-style-type: none"> <li>1. Absorber 1 column inlet,</li> <li>2. Absorber 2 column inlet,</li> <li>3. Water wash column inlet,</li> <li>4. Water wash outlet;</li> <li>5. Desorber outlet after reflux condenser</li> </ol>
Liquid titrations	Mettler Toledo auto titrator <ol style="list-style-type: none"> <li>1. Fast loop sampling from Abs 1 (Rich), Abs 2 (Semi-rich) and Desorber (Lean)</li> <li>2. MEA solvent concentration</li> </ol>

	3. CO <sub>2</sub> concentration and loading
Dissolved oxygen analysis	Jumo online oxygen analysis 1. Lean (desorber outlet) 2. Semi-rich (absorber 2 outlet) 3. Rich (absorber 1 outlet)
Iron analysis	Analysis on • Lean (desorber outlet)

### 3.2 Accelerated degradation tests in TERC

Test campaigns performed at TERC to investigate accelerated degradation are summarised below in Table 6. Samples were collected for post analysis during the tests which were analysed at SINTEF.

**Table 6: Overview of campaigns for accelerated degradation investigations**

Campaign #	Description	Duration (h)	Name	Comment
2*	40 wt% MEA	150	Higher O <sub>2</sub> /MEA	
3	128 °C (0.5 bar)	150	Higher O <sub>2</sub> /stripping T	
4	NO <sub>x</sub> injection	150	Higher O <sub>2</sub> /NO <sub>x</sub>	15 ppmv
5	Reduced oxygen 8%	150	Baseline	

\*Starting from 2, assuming that the long campaign described in D4.1.1. is Campaign 1 *Higher O<sub>2</sub>*.

For Campaign #3, stripper temperature was 128 °C due to system limitations at TERC, instead of 130 °C which was used in LAUNCH rig#2. The campaign showed the lowest degradation at TERC which is thought to be due to lower lean loading than in the rest of the campaigns, as a result of higher stripper temperature. This is in-line with literature findings regarding thermal degradation, showing that at higher loadings, thermal degradation is faster (Davis, 2009; Høisæter et al., 2022).

#### 3.2.1 Operation

The plant was drained of used MEA and washed with demineralised water before each test campaign. Fresh MEA was loaded into the plant for each test for comparison of results. All the test campaigns were performed with 35 wt% MEA except Campaign #2 which was performed with 40 wt% MEA. Control system of the plant maintains MEA concentration by periodic top up with water from water wash to absorber 1. The top up is tuned to transfer a very low amount of water (1-2 L) at a time which is relatively negligible (0.4%) in comparison with the total plant inventory (~500 L) so that overall concentration is not significantly affected. The main information, such as flows, temperatures, pressures, are presented for each campaign in Table 7. Details regarding the set-up and procedure used during the Higher O<sub>2</sub>/NO<sub>x</sub> campaign, where NO<sub>x</sub> is added as NO<sub>2</sub>, are given in Appendix B.

**Table 7: TERC operation parameters (mean values)**

Parameter	Unit	Campaign #2	Campaign #3	Campaign #4	Campaign #5
Temperature Gas inlet	°C	15	14	32	14
Pressure Gas inlet	mbarg	30	30	30	30
Inlet flowrate wet total	m <sup>3</sup> /h	190	190	190	190
Gas inlet composition, CO <sub>2</sub>	vol(%) dry	5.2	5.1	5.2	5.15
Gas inlet composition, NO <sub>x</sub>	vol(%) dry	0	0	15	0
Gas inlet composition, O <sub>2</sub>	vol(%) dry	19.5	19.5	19.5	8
Gas inlet composition, H <sub>2</sub> O	vol(%)	1	0.8	0.91	1

Lean solvent inlet temperature	°C	40	40	40	40
Lean solvent inlet flowrate	kg/h	300	300	300	300
Lean solvent density	kg/m <sup>3</sup>	1087	1023	1063	1072
Lean solvent inlet flowrate	L/h	276	293.3	282.2	280
Rich solvent outlet flowrate	kg/h	312	312	313	313
Rich solvent density	kg/m <sup>3</sup>	1123	1062	1101	1112
Rich solvent outlet flowrate	m <sup>3</sup> /h	278	293.8	284.3	281.5
Absorber 2 (Top)	°C	41	35	53	49
Absorber 2	°C	43	34	54	50
Absorber 2	°C	45	30	53	49
Absorber 2	°C	45	29	52	48
Absorber 2	°C	45	27	54	48
Absorber 2	°C	45	26	51	50
Absorber 2	°C	44	27	50	45
Absorber 2	°C	43	28	48	42
Absorber 2	°C	42	30	47	40
Absorber 2	°C	37	33	42	35
Absorber 2 (bottom)	°C	31	35	39	30
Absorber 1 (Top)	°C	34	45	40	30
Absorber 1	°C	40	53	41	32
Absorber 1	°C	41	55	40	33
Absorber 1	°C	39	55	38	31
Absorber 1	°C	36	55	37	29
Absorber 1	°C	34	55	35	27
Absorber 1	°C	33	55	34	27
Absorber 1	°C	31	53	32	26
Absorber 1	°C	29	50	31	23
Absorber 1	°C	25	44	29	20
Absorber 1 (bottom)	°C	38	40	40	34
Liquid volume in absorber sump	m <sup>3</sup>	0.07	0.07	0.07	0.07
Residence time in the absorber sump	min	14	14	14	14
Gas outlet temperature	°C	23	23	35	27
stripper T profile (top)	°C	87	114	86	87
stripper T profile	°C	77	111	83	86
stripper T profile	°C	99	117	103	103
stripper T profile	°C	100	117	104	104
stripper T profile (bottom)	°C	112	119	113	112
Liquid volume in reboiler	litres	450	450	450	450
Residence time in reboiler	min	90	90	90	90
Temperature in reboiler liquid	°C	118	120	118	118
Temp CO <sub>2</sub> product from condenser	°C	16	15	20	15
Cold rich inlet temperature	°C	14	19	24	14
Cold lean outlet temperature	°C	28	33	39	29
Hot rich outlet temperature	°C	57	64	77	68
Hot lean inlet temperature	°C	85	94	90	88

Table 8 shows loadings and capture efficiency data for the accelerated test campaign at TERC. All of the test campaigns has ~90% capture except two test campaign, higher stripper temperature (99%) and higher MEA concentration (94%).

**Table 8: Overview of loadings, cyclic capacity and capture rates at TERC**

Campaign	Lean loading (mean)	Rich loading (mean)	Cyclic capacity	Capture rate (gas side)
	mol CO <sub>2</sub> /mol MEA			%
1	0.19	0.41	0.22	90
2	0.17	0.36	0.19	94
3	0.11	0.37	0.24	99
4	0.18	0.40	0.22	90
5	0.19	0.39	0.2	89

### 3.2.2 Analytical measurements

A GasMET DX4000 FTIR is used for gas analysis, which sequentially tests samples from each of the locations. The entire sampling system from the plant to the FTIR including heated filters, heated sampling lines and a heated cabinet housing solenoid for sample switching is heated up to 180°C to avoid condensation. The sequence and sampling time is user defined and can be changed in the FTIR software as and when required. For these tests, gas compositions at Absorber 1 inlet and Absorber 2 outlet were used for overall capture efficiency calculations.

Solvent analysis is performed by an in-line and offline measurements. For online analysis, Mettler Toledo auto-titrator shown in Figure 7 is used. The apparatus collects three solvent samples (rich, lean and semi-rich). The fast sampling closed loop keeps a small bleed stream of solvent in circulation in respective stream and peristaltic pumps are used to acquire samples when needed. The auto-titrator performs titrations on the three samples for solvent concentration and CO<sub>2</sub> loading analysis. Offline measurements were performed for Fe analysis. Lean samples collected by the auto-titrator were used for Fe analysis using colorimetric method using the apparatus shown in Figure 8.



**Figure 7: Mettler Toledo auto-titrator**

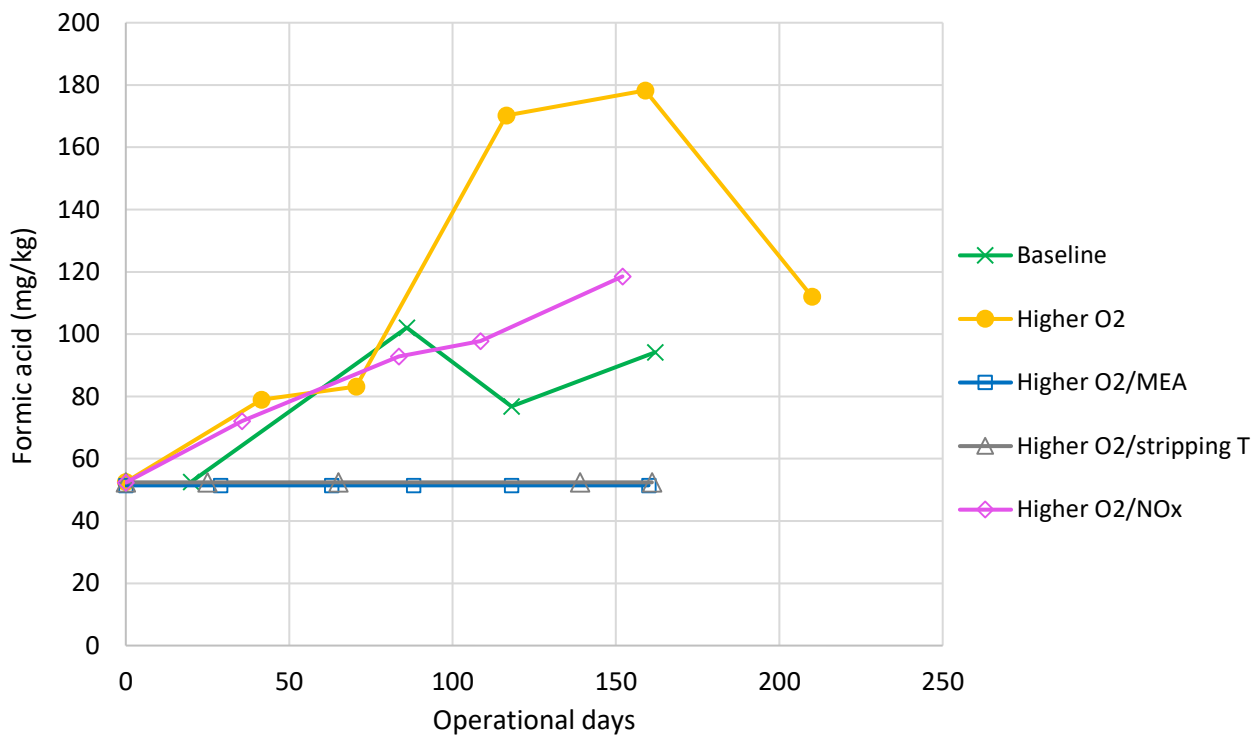


**Figure 8: Fe measurement apparatus**

A selection of samples was sent to SINTEF for analysis of degradation products. Analysis for the degradation products using Liquid chromatography–Mass spectrometry (LC-MS) was performed while Total Inorganic Carbon–Total Organic Carbon (TIC-TOC) method was used for the measurement of CO<sub>2</sub> in a selection of samples for comparison purposes.

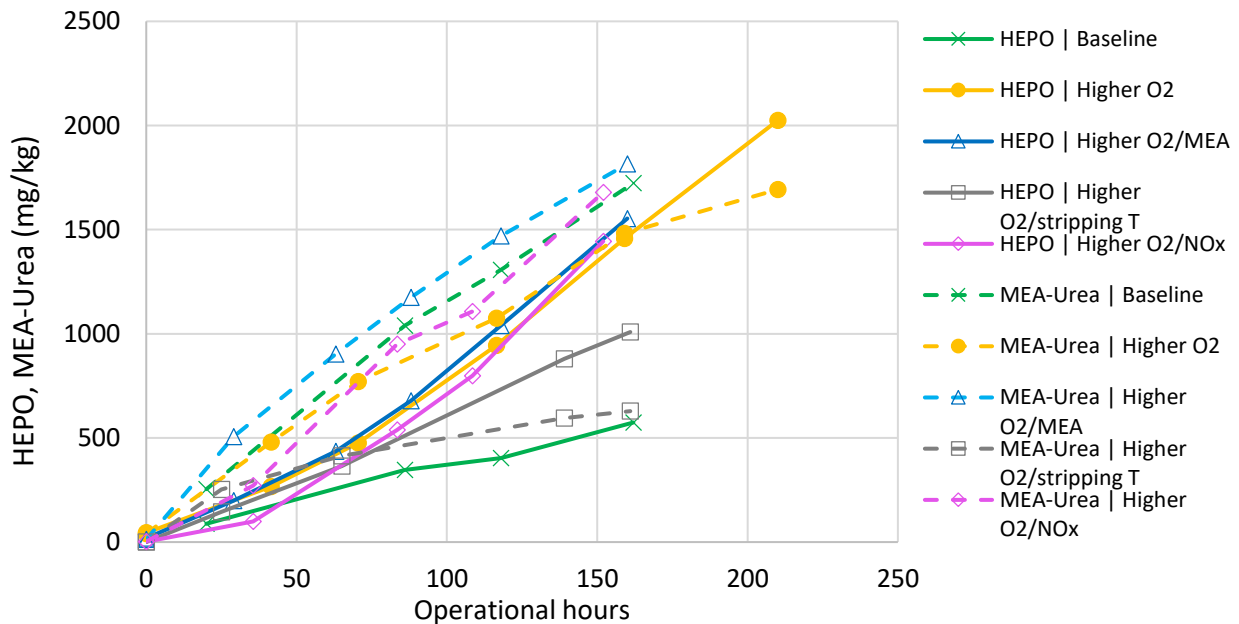
Figure 9 presents formic acid build up on CO<sub>2</sub> free basis during the accelerated degradation test campaigns at the TERC plant. For two of the test campaigns, the *Higher O<sub>2</sub>/stripping T* and *Higher O<sub>2</sub>/MEA*, the level of formic acid in the solvent samples was below the detection limit of the instrument (<50 mg/kg). This can be witnessed from the graph as a straight line along 50 mg/kg (52.6 mg/kg when corrected for CO<sub>2</sub>). Formic acid was quantified in the samples from the LAUNCH rig#2 from the start of the campaigns at <3 mg/kg. The measurements for the acids were conducted in TNO's analytical laboratory for the LAUNCH rig#2 and in SINTEF's analytical laboratory for TERC, thus explaining why the detection limits are different, i.e. 50 mg/kg for TERC and <3 mg/kg for LAUNCH rig#2.

For the *Baseline*, the trend has shown a weird behaviour with increasing concentration at the start while the sample after 120 hours of operation has shown a drop which could be due to measurement error. Further, formic acid is higher in the *Higher O<sub>2</sub>/NO<sub>2</sub>* injection case as compared to the *Baseline*, in agreement with the observations made in the LAUNCH rig#2. Overall, the acids that were analysed are in the same order of magnitude for both plants



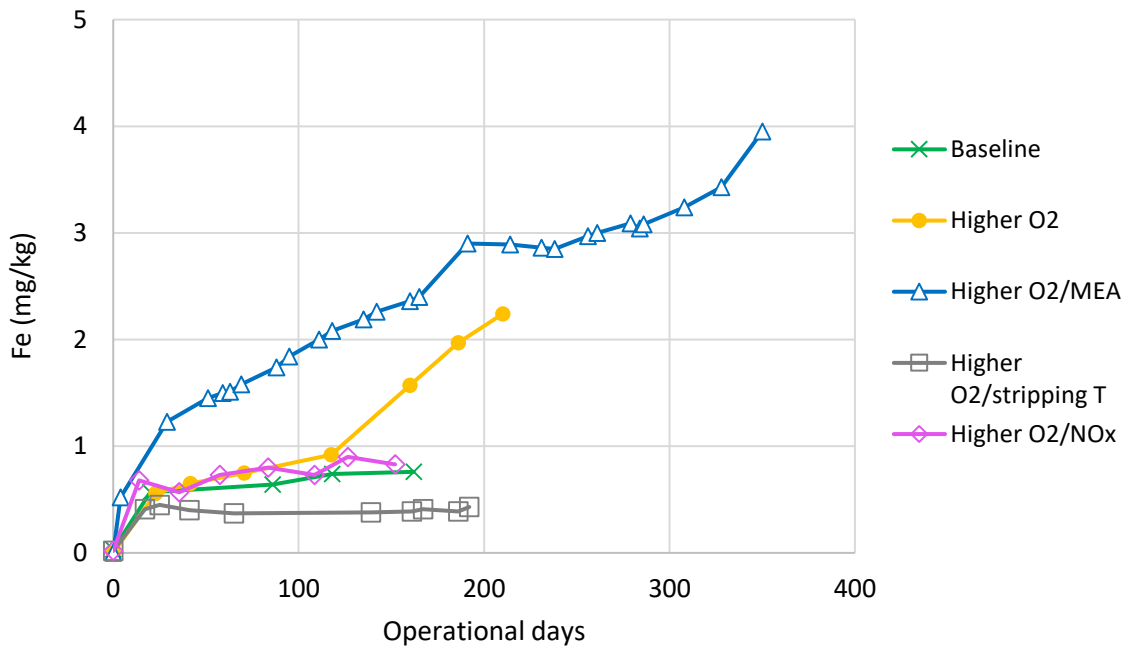
**Figure 9: Formic acid expressed in CO<sub>2</sub>-free basis during the accelerated degradation campaigns in TERC**

Figure 10 presents HEPO and MEA-Urea build up on CO<sub>2</sub> free basis during the accelerated degradation test campaigns at the TERC plant. The figure shows that the *Higher O<sub>2</sub>* and *Higher O<sub>2</sub>/MEA* (40 wt%) campaigns have the highest level of HEPO build up followed by *Higher O<sub>2</sub>/NO<sub>x</sub>*, *Higher O<sub>2</sub>/stripping T* while *Baseline* campaign has shown the lowest. For MEA-Urea, the higher concentration is shown again at the *Higher O<sub>2</sub>/MEA*, this time followed by the *Baseline* (8% O<sub>2</sub>), *Higher O<sub>2</sub>* and *Higher O<sub>2</sub>/NO<sub>x</sub>* campaigns, and last the *Higher O<sub>2</sub>/stripping T*. The third most dominant component is HeGly, which was also identified in the LAUNCH rig#2.



**Figure 10: HEPO (continuous lines) and MEA-Urea (dashed lines) concentration expressed in CO<sub>2</sub>-free basis during the accelerated degradation campaigns in TERC**

The iron concentration (CO<sub>2</sub> free basis) during the accelerated degradation campaigns is depicted in Figure 11. The higher Fe accumulation is shown for the *Higher O<sub>2</sub>/MEA*, followed by *Higher O<sub>2</sub>/NO<sub>2</sub>* and *Baseline* while *Higher O<sub>2</sub>/stripping T* campaign has shown the lowest. This is contrary of what has been observed in the LAUNCH rig#2, where the highest rate was seen for the *Higher O<sub>2</sub>/stripping T* campaign. This can be attributed to lower lean loadings achieved during the campaign as a results of higher temperature as pressure in the stripper was not changed as well as the fact that in TERC, iron was analyzed using a colorimetric method in comparison to Inductively-coupled plasma mass spectrometry (ICP-MS) used in LAUNCH rig#2. Different trends between the two rigs can be the result of using two different measuring techniques, with the colorimetric method being more prone to higher uncertainties due to the potential connection of the solvent color with degradation.



**Figure 11: Iron concentration expressed in CO<sub>2</sub>-free basis during the accelerated degradation campaigns in TERC**

## 4 Main findings from the LAUNCH rigs' campaigns

Different accelerated degradation techniques were tested, and the results were compared between TERC pilot plant (1000 kg CO<sub>2</sub>/day) and the LAUNCH rig (25 kg CO<sub>2</sub>/day). Overall, the LAUNCH rig was capable of matching the major degradation components found in the larger TERC pilot plant. Longer tests and differences in operating conditions can possibly explain the differences seen in the degradation trends, plus possibly the different metal contents as the run progresses. The main findings are discussed in this section.

Four accelerating degradation techniques were tested: increased oxygen levels in the flue gas, increased solvent concentration, increased stripping temperature, and addition of NO<sub>x</sub>. Increasing the MEA content in the solvent, the stripping temperature and the addition of NO<sub>x</sub> was studied in combination with increased O<sub>2</sub> content in the gas. The acids that were analysed for both plants are in general in the same order of magnitude for both plants (except for acetic acid which was not detected in the LAUNCH rig#2 campaigns), with formic acid being the most dominant one. Major degradation products are HEPO, MEA-Urea and HeGly in both LAUNCH rig and TERC, which is in agreement with work performed earlier in another LAUNCH rig (Vevelstad et al., 2017). HEPO is the most dominant degradation product of them, followed by MEA-Urea in almost all cases, and are used to assess the effectivity of the different strategies to accelerate degradation.

Increasing the oxygen content in the flue gas from 7 vol% to 18 vol% clearly accelerates degradation. The *Baseline* campaign with 7 vol% O<sub>2</sub> shows lower concentration for both degradation products and metals when compared to the *Increased O<sub>2</sub>* campaign. Although the *Increased O<sub>2</sub>* campaign in the LAUNCH rig#2 had a higher Fe starting concentration, which is expected to have also contributed to the degradation progression in the solvent, it is seen that the *Baseline* campaign has the lowest degradation products concentration of all the campaigns, demonstrating that *Increasing O<sub>2</sub>* content in the flue gas is a successful technique for accelerating degradation. In the TERC campaigns, the *Baseline* campaign shows also the lowest concentration of organic degradation compounds, and specifically the most dominant ones HEPO and MEA-Urea. However, the *Higher O<sub>2</sub>/MEA* and *Higher O<sub>2</sub>/stripping T* campaigns had lower formic acid concentration than the *Baseline*, the reason for which is not clear.

Increasing the MEA content of the solvent does not seem to have a strong influence on the acceleration of the oxidative degradation products (acids), although it has an increasing effect on the metal accumulation seen in the studied systems. The *Higher O<sub>2</sub>/MEA* campaign yields the highest concentration of HEPO and MEA-Urea, according to the results from TERC. In the LAUNCH rig#2, such trend is not shown, however the reason for this might be the lower MEA concentration (~37 wt% MEA) compared to TERC (~40 wt% MEA), as a result of water imbalance in the system and thus difficulty to control the solvent composition. Regarding metals, in TERC, the iron content is higher than in the rest of the campaigns, though it is noted that the iron method used in this work is a colorimetric method, which is more prone to higher uncertainties due to the potential connection of the solvent color with degradation. In the LAUNCH rig#2, the iron content is generally higher in the *Higher O<sub>2</sub>/MEA* campaign, though it is exceeded towards the end of the campaigns in the case of *Higher O<sub>2</sub>/stripping T*.

Increasing the stripping temperature does not seem to affect the formation of oxidative degradation products, meaning formic and oxalic acid, while it led to the highest concentrations of HEPO and MEA-Urea and metal accumulation in the system compared to the rest of the campaigns. These trends are demonstrated with the LAUNCH rig#2. A comparison and drawing conclusions based on the TERC results is more challenging due to the facts that, first, the temperature was increased to 128 °C in TERC (instead of 130 °C) and, mainly, because the stripping pressure remained the same, thus leading to lower loadings than in the rest of the campaigns, making the comparison invalid (although reflecting likely industrial practice, in having higher stripper temperature associated with a lower lean loading).

The effectivity of adding NO<sub>x</sub> in the flue gas as an accelerating degradation technique is shown to be dependent on the level of NO<sub>x</sub> added and the degradation product targeted. Tests in the LAUNCH rig#2 with 169 ppmv show a sharp increase in the formation of acids, specifically formic acid, while the HEPO and MEA-Urea concentration were at the same level as the *Increased O<sub>2</sub>* campaign. Metals also remained at the same level as the *Baseline*. Tests in TERC were conducted with 15 ppmv, which is much lower than in the LAUNCH rig#2 and more representative of industrial flue gases. The campaign with *Increased O<sub>2</sub>/NO<sub>x</sub>* showed higher



formic acid concentration than the other campaigns, but no higher than the *Increased O<sub>2</sub>* one. No clear effect is shown when comparing HEPO and MEA-Urea products, since HEPO concentration by the end of the campaign is similar to the *Increasing O<sub>2</sub>/MEA* campaign, which yielded the higher concentration, while MEA-Urea concentration is lower than the *Baseline* campaign. The metal concentration was similar to the *Baseline* campaign, in agreement with LAUNCH rig#2 findings.

Looking at specific degradation products, it is seen that formic acid is the most dominant acid and it is seen at highest concentration for both plants in the *Increased O<sub>2</sub>* campaign. One would expect that higher formic acid concentration would be seen during the accelerated degradation campaigns where either MEA/stripping T or NO<sub>x</sub> concentration is increased, while the oxygen content is the same. As far as the LAUNCH rig#2 is concerned, the starting solvent already contained some iron, which can explain the above observation. Interestingly, the second most dominant acid in TERC was acetic acid, which was actually not identified in the LAUNCH rig#2 campaigns. Moreover, the *Baseline* campaign has the lowest concentration in the LAUNCH rig while it is under detection limit for the *Higher O<sub>2</sub>/MEA* and *Higher O<sub>2</sub>/stripping T* campaigns in TERC.

As also mentioned before, major degradation products are HEPO, MEA-Urea and HeGly in both LAUNCH rig and TERC. HEPO and MEA-UREA are highest at *Higher O<sub>2</sub>/stripping T* campaign in the LAUNCH rig and at *Higher O<sub>2</sub>/MEA* in TERC.

The concentration of metals was also measured since not only can they provide insights regarding the corrosivity of the system, but also because literature on solvent management generally agrees that the metals' content in the solvent is a key determinant aspect of the degradation rate. In the LAUNCH rig#2, several metals were analyzed for by ICP-MS (Cr, Fe, Ni, Mn, Cu, Zn, Mo, Ba, Pb). They were all below 2 mg/kg after approximately 350 hours of operation, except for Fe and Zn that were seen in higher concentrations. Iron was the highest, while the Zn concentration profile always followed the same trend (ending at 2-3 mg/kg concentration). Iron was seen building up in the solvent in a much higher rate during the *Higher O<sub>2</sub>/stripping T* campaign than in the rest of the accelerated degradation campaigns. In TERC, iron found to be the highest during the *Higher O<sub>2</sub>* and *Higher O<sub>2</sub>/MEA* campaigns in TERC. These different trends between the two rigs is believed to be the result of using two different measuring techniques (ICP-MS and colorimetric method, as explained earlier).

Although it is seen that the LAUNCH rig#2 is capable of predicting the degradation trends and the most significant degradation products as larger rigs, such as TERC, it is noted that when comparing the trends between the two rigs, we see significant differences regarding the accelerated degradation strategy that yields higher degradation. We see the increased O<sub>2</sub> having a general accelerating affect, and after this higher stripping T is shown more influential in the LAUNCH rig, while higher wt% MEA is more pronounced in TERC. This could be the result of performing the campaigns in not exactly the same parameters and conditions. During the *Higher O<sub>2</sub>/MEA* campaigns, the composition of the solvent was slightly more concentrated (~37 wt%) due to dilution in the LAUNCH rig#2, while it was 40 wt% in TERC. In addition, while the *Higher O<sub>2</sub>/stripping T* in the LAUNCH rig#2 was 130°C, 128°C was used in TERC due to system limitations. For the latter, the stripping pressure, and thus the loadings of the solvent also differed, making a direct comparison impossible.

## 5 Evaluation of result using the DNM model

DNM stands for Degradation Network Model and it is presented in the LAUNCH report *D1.3.4 Degradation Network model*. In this work, the model is used to assess the representativeness of DNM in comparison to the results from the demonstration campaigns. The model predicts the amine consumption by its reaction with oxygen, and not the specific type and amount of degradation products. Therefore, the LAUNCH rig #2 results from Campaign #2 *Increased O<sub>2</sub>/MEA* (~37 wt% MEA, 19.8 vol% O<sub>2</sub> in inlet flue gas, dry basis) and from Campaign #5 *Baseline* (~34 wt% MEA, 7.6 vol% O<sub>2</sub> in inlet flue gas, dry basis) are used in the evaluation due to their difference in flue gas oxygen concentration. It is noted that the model is validated against data from 30 wt% MEA, however, its results are evaluated in this work for its applicability in ~35 wt% MEA systems.

The model requires input on temperature profile in the absorber, residence time and loading of the solvent in the sump and along the absorber. Since liquid hold-up and loading along the packing of the absorber is not available from the experimental data, simulation work was performed for their calculations. The dimensions of the absorber and process parameters (flowrate, temperature, pressure) were used in order to simulate the process and predict the lean and rich loadings. During the analysis, it was found that the predicted lean and rich loadings do not match the experimental ones. Looking in Table 3, it can be seen that indeed for the campaigns chosen for this work, although they had very similar rich loading after the absorber sump, 0.44-0.45, and the lean was 0.27-0.28 mol CO<sub>2</sub>/mol amine, a larger deviation is seen in the calculation of the capture rate, indicating uncertainty in one of the two values. Since the rich loading was more consistent throughout the campaigns, as witnessed in Table 3, it was decided to match the rich loading during the simulation work. This was done by adjusting the boil-up ratio in the reboiler, to produce a lean solvent which would lead to the experimental rich loading. Based on the above, the model predicted the MEA consumption in mol/h along the campaign.

The comparison is made with the oxidative degradation products, as presented in sub-section 2.2.2, and (average) ammonia emissions, as presented in Table 2. The components that are included in this analysis are, therefore, ammonia, formic acid, acetic acid, oxalic acid, nitric acid and nitrous acid. The corresponding MEA consumption calculation is based on the stoichiometry of the MEA reactions to the chosen degradation products, as reported in the work of Vevelstad et al. (Vevelstad et al., 2010). Specifically, the stoichiometry used for MEA with formic acid, acetic acid and oxalic acid is 1:1. In the proposed reactions, ammonia is produced together with compounds that are analysed in this work as well as others which are not analysed. For the analysed ones, ammonia is also produced with acetic acid and oxalic acid (1 mol of MEA producing 1 mol of acid and 1 mol ammonia). For the non-analysed ones, ammonia is produced together with formaldehyde, acetaldehyde, glycolic acid, hydroxy-acetaldehyde, glyoxylic acid and other more known and unknown components. Therefore, from the total mol of ammonia produced, the mol of acetic acid and oxalic acid are subtracted so as they are not double counted. In addition, nitrates and nitrites are the result of ammonia reaction with oxygen (NH<sub>3</sub>:HNO<sub>3</sub>/HNO<sub>2</sub>, 1:1), therefore, and similar to the acids above, the mol of nitric acid and nitrous acid are subtracted from the total calculated mol NH<sub>3</sub> in order not to double-count the MEA consumption. As a result, the remaining amount of ammonia is connected to different degradation products than formic, acetic, oxalic, nitric and nitrous acids. The result of this analysis is the total amount of mol of degradation products, which is equal to the mol of MEA consumed.

The results are listed in

Table 9. The results are calculated for the intervals at which new samples were withdrawn, in order to evaluate whether in the start of the campaigns, the model predicts more accurately the results due to lower degradation degree and/or degradation products' number. It is interesting to know that the amount of measured degradation products formation is mainly attributed to the amount of ammonia produced which corresponds to more than 90% of the total value.

The model captures the general trend of the results, since it predicts that the degradation for the higher oxygen campaign is higher than in the lower oxygen campaign, which is also seen in the experimental results. The model consistently underpredicts the degree of oxidative degradation for both campaigns, while for each campaign, the level of relative deviation (RD) remains approximately the same along the campaign. The latter indicates that the amount of degradation which is not accounted for in the model in the start of the campaign

is the same in its end, thus the reason of deviation is probably not the change in degradation rate or additional degradation products that are formed in an higher degree with increasing operating hours. The predicted values are of the same order of magnitude or with one order difference as the measured ones. In the high oxygen campaign (#2) RD = -76% and, in the lower oxygen campaign (#5), RD = -30%. Hence, the model yields better results for the lower oxygen case.

**Table 9: Comparison measured and modelled values with the DNM model.**

Operating time	MEA consumption modelled	Estimated MEA consumption based on measured degradation products formation*	RD**
h	mol	mol	%
Campaign #2 – 19.8 vol% O <sub>2</sub>			
96	0.08	0.34	-77
216	0.17	0.73	-77
288	0.23	0.97	-76
384	0.31	1.29	-76
456	0.36	1.53	-76
528	0.42	1.77	-76
Campaign #5 – 7.6 vol% O <sub>2</sub>			
24	0.01	0.02	-29
96	0.06	0.08	-29
192	0.12	0.17	-31
264	0.16	0.23	-30
360	0.22	0.31	-30

\* The total amount of mol of degradation products is equal to the mol of MEA consumed, based on the stoichiometries according to (Vevelstad et al., 2010).

\*\*relative deviation:  $(X_{\text{model}} - X_{\text{meas}}) / X_{\text{meas}} \%$

The demonstration results show that degradation was more accelerated than predicted by the model, especially for the case of increased oxygen content in the flue gas. The model in its current form cannot capture the impact of increased oxygen concentration as a result of having developed a model which is “calibrated” with degradation data from real operation of a CO<sub>2</sub> capture pilot plant with 30 wt% MEA and with specific oxygen content in the flue gas. Other limitations are the fact that it was not possible to match both lean and rich loadings, that the measurement of ammonia emissions has high uncertainty since the average measurement along the campaign is used, as well as that the solvent exhibited metal accumulation along the campaign, which can affect the degradation profiles and they are not taken into account into the model. For example, 5 mg/kg of iron were measured in the end of high oxygen campaign, while 1 mg/kg of iron was measured in the low oxygen one.

## 6 Conclusions

Different accelerated degradation techniques were tested, and the results were compared between TERC pilot plant (1000 kg CO<sub>2</sub>/day) and the LAUNCH rig (25 kg CO<sub>2</sub>/day). Four accelerating degradation techniques were tested: increased oxygen levels in the flue gas, increased solvent concentration, increased stripping temperature, and addition of NO<sub>x</sub>. Increasing the MEA content in the solvent, the stripping temperature and the addition of NO<sub>x</sub> was studied in combination with increased O<sub>2</sub> content in the gas.

The major degradation products were HEPO, MEA-Urea and HEGly, while formic acid was the most dominant acid. Iron concentrations up to 4 mg/kg were seen in TERC and up to 7 mg/kg in the LAUNCH rig#2. In addition, the concentration of zinc (Zn - a known degradation catalyst) in LAUNCH rig#2 was possibly significant, sometimes exceeding the Fe concentration; the source of it is suspected to be a heating element in the rig. Zinc and copper construction materials would not normally be expected to be included in the wetted path of amine capture plants. Although it is seen that the LAUNCH rig#2 is capable of predicting the degradation trends and the most significant degradation products as larger rigs, such as TERC, it is noted that when comparing the trends between the two rigs, we see significant differences regarding the accelerated degradation strategy that yields higher degradation. For example, highest HEPO, MEA-Urea and Fe concentration were found at the *Higher O<sub>2</sub>/stripping T* campaign in the LAUNCH rig, while this was the case for *Higher O<sub>2</sub>/MEA* campaign at TERC. The campaigns were performed with the two rigs in similar, but not identical, conditions, therefore longer tests and more similar operating conditions can possibly explain the differences seen in the degradation trends, as explained below.

Overall, increasing the oxygen content in the flue gas from 7 vol% to 18 vol% clearly accelerates degradation. The *Baseline* campaign with 7 vol% O<sub>2</sub> shows lower concentration for both degradation products and metals when compared to the *Increased O<sub>2</sub>* campaign. Although the *Increased O<sub>2</sub>* campaign in the LAUNCH rig#2 had a higher Fe starting concentration, which is expected to have also contributed to the degradation progression in the solvent, it is seen that the *Baseline* campaign has the lowest degradation products concentration of all the campaigns, demonstrating that *Increasing O<sub>2</sub>* content in the flue gas is a successful technique for accelerating degradation. In the TERC campaigns, the *Baseline* campaign shows also the lowest concentration of organic degradation compounds, and specifically the most dominant ones HEPO and MEA-Urea. However, the *Higher O<sub>2</sub>/MEA* and *Higher O<sub>2</sub>/stripping T* campaigns had lower formic acid concentration than the *Baseline*, the reason for which is not clear.

Increasing the MEA content of the solvent does not seem to have a strong influence on the acceleration of the oxidative degradation products (acids), although it has an increasing effect on the metal accumulation seen in the studied systems. The *Higher O<sub>2</sub>/MEA* campaign yields the highest concentration of HEPO and MEA-Urea, according to the results from TERC. In the LAUNCH rig#2, such trend is not shown, however the reason for this might be the lower MEA concentration (~37 wt% MEA) compared to TERC (~40 wt% MEA), as a result of water imbalance in the system and thus difficulty to control the solvent composition. Regarding metals, in TERC, the iron content is higher than in the rest of the campaigns, though it is noted that the iron method used in this work is a colorimetric method, which is more prone to higher uncertainties due to the potential connection of the solvent color with degradation. In the LAUNCH rig#2, the iron content is generally higher in the *Higher O<sub>2</sub>/MEA* campaign, though it is exceeded towards the end of the campaigns in the case of *Higher O<sub>2</sub>/stripping T*.

Increasing the stripping temperature does not seem to affect the formation of oxidative degradation products, meaning formic and oxalic acid, while it led to the highest concentrations of HEPO and MEA-Urea and metal accumulation in the system compared to the rest of the campaigns. These trends are demonstrated with the LAUNCH rig#2. A comparison and drawing conclusions based on the TERC results is more challenging due to the facts that, first, the temperature was increased to 128 °C in TERC (instead of 130 °C) and, mainly, because the stripping pressure remained the same, thus leading to lower loadings than in the rest of the campaigns, making it the comparison invalid.

The effectivity of adding NO<sub>x</sub> in the flue gas as an accelerating degradation technique is shown to be dependent on the level of NO<sub>x</sub> added and the degradation product targeted. Tests in the LAUNCH rig#2 with 169 ppmv show a sharp increase in the formation of acids, specifically formic acid, while the HEPO and MEA-



Urea concentration were at the same level as the *Increased O<sub>2</sub>* campaign. Metals also remained at the same level as the *Baseline*. Tests in TERC were conducted with 15 ppmv, which is much lower than in the LAUNCH rig#2 and more representative of industrial flue gases. The campaign with *Increased O<sub>2</sub>/NO<sub>x</sub>* showed higher formic acid concentration than the other campaigns, but no higher than the *Increased O<sub>2</sub>* one. No clear effect is shown when comparing HEPO and MEA-Urea products, since HEPO concentration by the end of the campaign is similar to the *Increasing O<sub>2</sub>/MEA* campaign, which yielded the higher concentration, while MEA-Urea concentration is lower than the *Baseline* campaign. The metal concentration was similar to the *Baseline* campaign, in agreement with LAUNCH rig#2 findings.

Regarding the assessment of representativeness of the DNM model, its predictions were compared with the experimental results of two campaigns; one with ~37 wt% MEA and 19.8 vol% O<sub>2</sub>, and one with ~34 wt% MEA and 7.6 vol% O<sub>2</sub> in the flue gas (dry basis). The model captures the general trend of the results, by predicting that the degradation for the higher oxygen campaign is higher than in the lower oxygen campaign, which is also seen in the experimental results. The model consistently underpredicts the degree of oxidative degradation for both campaigns, while for each campaign, the level of relative deviation (RD) remains approximately the same along the campaign. In the high oxygen campaign, the relative deviation between the predicted and measured values is -76% and, in the lower oxygen campaign, it is -30%. Hence, the model yields better results for the lower oxygen case. This points towards the fact that the model is developed and "calibrated" with degradation data from real operation of a CO<sub>2</sub> capture pilot plant with specific oxygen content in the flue gas, as well as using 30 wt% MEA. Other sources of error are the high uncertainty in ammonia measurement, presence of additional oxidative and thermal degradation products as well as metals which are not accounted in the model.

## 7 References

- Chi, S., & Rochelle, G. T. (2002). Oxidative Degradation of Monoethanolamine. *Industrial and Engineering Chemistry Research*, 41(17), 4178–4186. <https://doi.org/10.1021/IE010697C>
- Davis, J. D. (2009). *Thermal degradation of aqueous amines used for carbon dioxide capture*. <https://repositories.lib.utexas.edu/handle/2152/6581>
- Fine Nathan. (2015). *Nitrosamine Management in Aqueous Amines for Post-Combustion Carbon Capture*.
- Han, J., Jin, J., Eimer, D. A., & Melaaen, M. C. (2012). Density of water (1) + monoethanolamine (2) + CO<sub>2</sub> (3) from (298.15 to 413.15) K and surface tension of water (1) + monoethanolamine (2) from (303.15 to 333.15) K. *Journal of Chemical and Engineering Data*, 57(4), 1095–1103. <https://doi.org/10.1021/je2010038>
- Høisæter, K. K., Vevelstad, S. J., Braakhuis, L., & Knuutila, H. K. (2022). Impact of Solvent on the Thermal Stability of Amines. *Industrial and Engineering Chemistry Research*, 61(43), 16179–16192. [https://doi.org/10.1021/ACS.IECR.2C01934/ASSET/IMAGES/LARGE/IE2C01934\\_0016.JPEG](https://doi.org/10.1021/ACS.IECR.2C01934/ASSET/IMAGES/LARGE/IE2C01934_0016.JPEG)
- Léonard, G., Voice, A., Toye, D., & Heyen, G. (2014). Influence of Dissolved Metals and Oxidative Degradation Inhibitors on the Oxidative and Thermal Degradation of Monoethanolamine in Postcombustion CO<sub>2</sub> Capture. *Industrial and Engineering Chemistry Research*, 53(47), 18121–18129. <https://doi.org/10.1021/IE5036572>
- Michailos, S. & Gibbins, J. (2022). *A Modelling Study of Post-Combustion Capture Plant Process Conditions to Facilitate 95–99% CO<sub>2</sub> Capture Levels From Gas Turbine Flue Gases*. *Frontiers in Energy Research* (10). <https://www.frontiersin.org/articles/10.3389/fenrg.2022.866838> ; DOI=10.3389/fenrg.2022.866838
- Morken, A. K., Pedersen, S., Nesse, S. O., Flø, N. E., Johnsen, K., Feste, J. K., de Cazenove, T., Faramarzi, L., & Vernstad, K. (2019). CO<sub>2</sub> capture with monoethanolamine: Solvent management and environmental impacts during long term operation at the Technology Centre Mongstad (TCM). *International Journal of Greenhouse Gas Control*, 82(January), 175–183. <https://doi.org/10.1016/j.ijggc.2018.12.018>
- Mullen, D. (2023) LAUNCH Reports D1.3.2 *Generalizing and Validating the DNM-LAUNCH rigs and pilot runs* and D1.3.3 *Optimised design and operation of capture units to reduce degradation*.
- Reddy, S., & Gilmatrin, J. (2008). Fluor's econamine FG PlusSM technology for post combustion CO<sub>2</sub> capture. *GPA Gas Treatment Conference*.
- Vevelstad, S. J., Eide-Haugmo, I., Falck Da Silva, E., & Svendsen, H. F. (2010). Degradation of MEA; a theoretical study. *Energy Procedia*. <https://doi.org/10.1016/j.egypro.2011.02.031>
- Vevelstad, S. J., Grimstvedt, A., Haugen, G., Kupfer, R., Brown, N., Einbu, A., Vernstad, K., & Zahlsen, K. (2017). Comparison of different Solvents from the Solvent Degradation Rig with Real Samples. *Energy Procedia*, 114, 2061–2077. <https://doi.org/10.1016/J.EGYPRO.2017.03.1341>

## Appendices

### Appendix A. Overview of components and analytical methods

**Table A-1: Overview of components analyzed in this work and corresponding analytical method**

Abbreviation	CAS	Name	Formula	Analysis method*
MEA	141-43-5	Monoethanolamine	C <sub>2</sub> H <sub>7</sub> N O	FT-IR <sup>1,2</sup> , IC <sup>1</sup> , LC-MS <sup>1,2</sup>
H <sub>2</sub> O	-	Water	H <sub>2</sub> O	FT-IR <sup>1,2</sup> , KF <sup>1</sup>
CO <sub>2</sub>	124-38-9	Carbon dioxide	CO <sub>2</sub>	FT-IR <sup>1,2</sup> , PA <sup>1</sup> , TIC-TOC <sup>1</sup>
Formic acid	64-18-6	Methanoic acid	C H <sub>2</sub> O <sub>2</sub>	IC <sup>1,2</sup>
Acetic acid	64-19-7	Ethanoic acid	C <sub>2</sub> H <sub>4</sub> O <sub>2</sub>	IC <sup>1,2</sup>
Oxalic acid	144-62-7	Ethanedioic acid	C <sub>2</sub> H <sub>2</sub> O <sub>4</sub>	IC <sup>1,2</sup>
Nitrate	14797-55-8	Nitrate	NO <sub>3</sub> <sup>-</sup>	IC <sup>1</sup>
Nitrite	14797-65-0	Nitrite	NO <sub>2</sub> <sup>-</sup>	IC <sup>1</sup>
HEEDA/AEEA	111-41-1	2-[(2-aminoethyl)amino]-ethanol	C <sub>4</sub> H <sub>12</sub> N <sub>2</sub> O	LC-MS <sup>1,2</sup>
HEHEAA	144236-39-5	N-(2-hydroxyethyl)-2-[(2-hydroxyethyl)amino]-acetamide	C <sub>6</sub> H <sub>14</sub> N <sub>2</sub> O <sub>3</sub>	LC-MS <sup>1,2</sup>
MEA urea	15438-70-7	N,N'-bis(2-hydroxyethyl)-urea	C <sub>5</sub> H <sub>12</sub> N <sub>2</sub> O <sub>3</sub>	LC-MS <sup>1,2</sup>
HEI	1615-14-1	1H-imidazole-1-ethanol	C <sub>5</sub> H <sub>8</sub> N <sub>2</sub> O	LC-MS <sup>1,2</sup>
HEF	693-06-1	N-(2-hydroxyethyl)-formamide	C <sub>3</sub> H <sub>7</sub> N O <sub>2</sub>	LC-MS <sup>1,2</sup>
OZD	497-25-6	2-oxazolidinone	C <sub>3</sub> H <sub>5</sub> N O <sub>2</sub>	LC-MS <sup>1,2</sup>
HEPO	23936-04-1	4-(2-hydroxyethyl)-2-piperazinone	C <sub>6</sub> H <sub>12</sub> N <sub>2</sub> O <sub>2</sub>	LC-MS <sup>1,2</sup>
HeGly	5835-28-9	N-(2-hydroxyethyl)-glycine	C <sub>4</sub> H <sub>9</sub> N O <sub>3</sub>	LC-MS <sup>1,2</sup>
BHEOX	1871-89-2	N <sub>1</sub> ,N <sub>2</sub> -bis(2-hydroxyethyl)-ethanediamide	C <sub>6</sub> H <sub>12</sub> N <sub>2</sub> O <sub>4</sub>	LC-MS <sup>1,2</sup>
HEA	142-26-7	N-(2-hydroxyethyl)-acetamide	C <sub>4</sub> H <sub>9</sub> N O <sub>2</sub>	LC-MS <sup>1,2</sup>
HEIA	3699-54-5	1-(2-hydroxyethyl)-2-imidazolidinone	C <sub>5</sub> H <sub>10</sub> N <sub>2</sub> O <sub>2</sub>	LC-MS <sup>1,2</sup>
2-oxazoline	504-77-8	4,5-dihydro-oxazole	C <sub>3</sub> H <sub>5</sub> N O	LC-MS <sup>1,2</sup>
NHEGly	80556-89-4	2-[(2-hydroxyethyl)nitrosoamino]-acetic acid	C <sub>4</sub> H <sub>8</sub> N <sub>2</sub> O <sub>4</sub>	LC-MS <sup>1,2</sup>
Cr	7440-47-3	Chromium	Cr	ICP-MS <sup>1</sup>
Fe	7439-89-6	Iron	Fe	ICP-MS <sup>1</sup>
Ni	7440-02-0	Nickel	Ni	ICP-MS <sup>1</sup>
Mn	7439-96-5	Manganese	Mn	ICP-MS <sup>1</sup>
Cu	7440-50-8	Copper	Cu	ICP-MS <sup>1</sup>
Zn	7440-66-6	Zinc	Zn	ICP-MS <sup>1</sup>
Mo	7439-98-7	Molybdenum	Mo	ICP-MS <sup>1</sup>
Ba	7440-39-3	Barium	Ba	ICP-MS <sup>1</sup>
Pb	7439-92-1	Lead	Pb	ICP-MS <sup>1</sup>

\*FT-IR: Fourier-transform Infrared Spectrometer, IC: Ion Chromatography, LC-MS: Liquid chromatography–Mass spectrometry, KF: Karl-Fischer titration, PA: Phosphoric acid, TIC-TOC: Total Inorganic Carbon-Total Organic Carbon, ICP-MS: Inductively coupled plasma mass spectrometry

<sup>1</sup>: LAUNCH rig #2, <sup>2</sup>: TERC

## Appendix B. NO<sub>x</sub> campaigns information

During Campaign #4, which was conducted in the presence of NO<sub>x</sub>, severe mist formation was observed in LAUNCH rig #2.

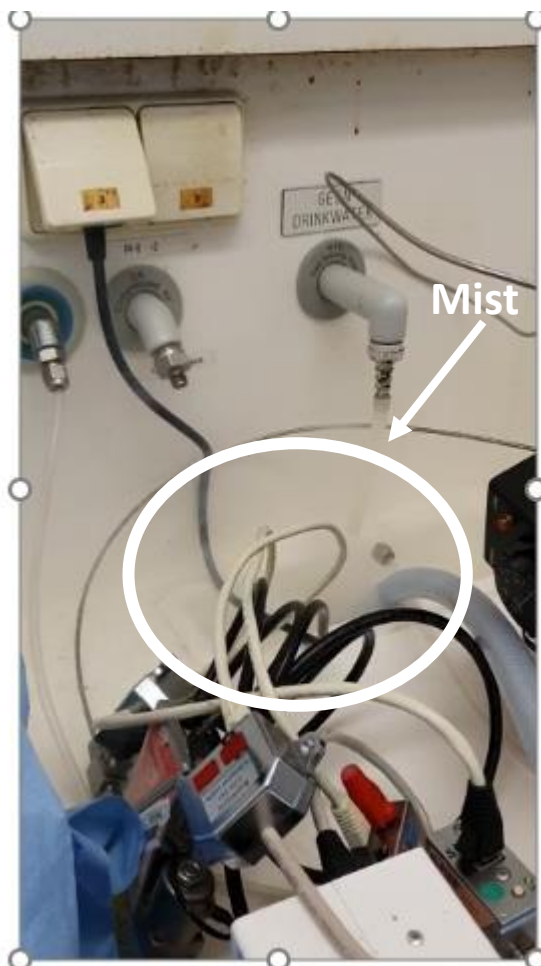


**Figure B. 1: Mist formation in the clean air outlet**

Regarding the NO<sub>x</sub> campaign at TERC, a mixture of air and CO<sub>2</sub> was used as flue gas. The air was sucked in by a blower. CO<sub>2</sub> from cryogenic storage tank, metered by gas mixing skid was injected into the air stream at the inlet side of the blower. In order to assess the impact of NO<sub>x</sub> on the solvent degradation, NO<sub>2</sub> was injected at rate of 15 ppmv (campaign 4). NO<sub>2</sub> was bought from BOC in 200 bar cylinders at 3000 ppm in air. A cost comparison was made for different NO<sub>2</sub> concentration and pressures and the above concentration and pressure was found to be the most suitable in terms of economics and personal safety. NO<sub>2</sub> detectors were used during the tests to detect leaks in the system (around the cylinder) and associated pipework.

For a gas flow rate of 190 m<sup>3</sup>/h into the absorber, ~ 20 cylinders were required to maintain a NO<sub>2</sub> concentration of 15 ppmv over the duration of the test campaign (150 hrs). NO<sub>2</sub> stream was injected into the mixed stream (air + CO<sub>2</sub>) upstream of the blower. The flow rate of the NO<sub>2</sub> stream was not measured but total flow rate of the flue gas stream was controlled to 190 m<sup>3</sup>/h via the PLC program using VSD control. NO<sub>2</sub> concentration was measured in the flue gas using FTIR at the inlet of the absorber. The figure below shows schematic of the set up used for NO<sub>2</sub> injection. Three cylinders connected in series were used to run the plant overnight. N<sub>2</sub> purge was provided to purge the lines before disconnected and connecting cylinders. Needle valves, shown

as blue in the diagram, were used to control the NO<sub>2</sub> stream to adjust the NO<sub>2</sub> concentration in the flue gas stream to the desired levels (15/5 ppm).

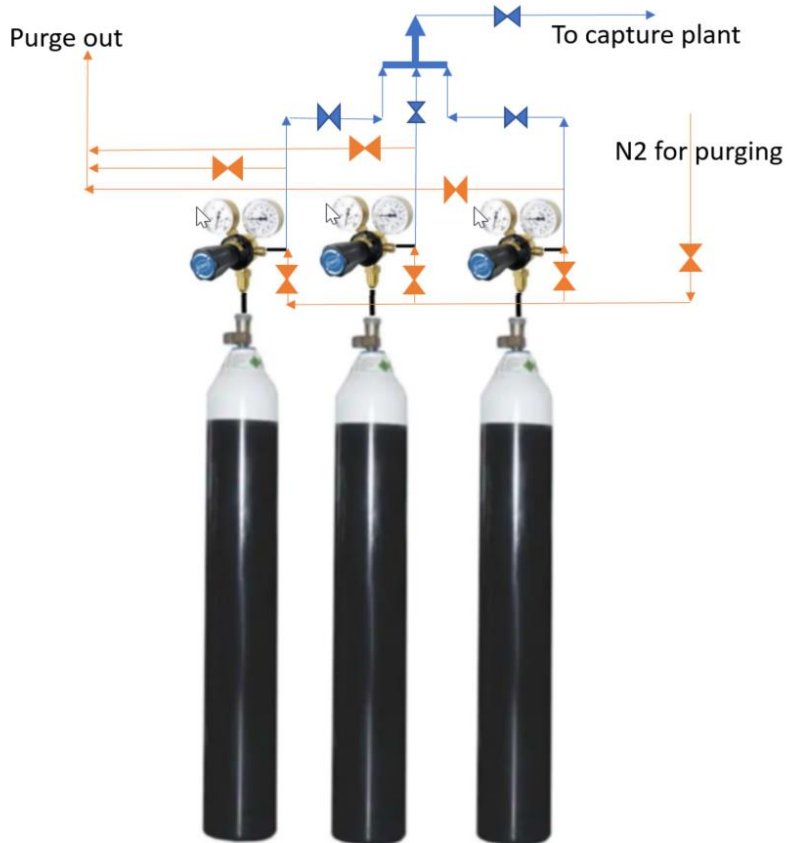


**Figure B. 2: NO<sub>2</sub> injection set-up at TERC**

## Appendix C. Analytical measurements

**Table C. 1: IC measurements for LAUNCH rig#2 campaigns**

Operational time hrs	IC						
	MEA	Ammonium	Acetic acid	Formic acid	Oxalic acid	Nitrate	Nitrite
	mg/kg	mg/kg	mg/kg	mg/kg	mg/kg	mg/kg	mg/kg
Campaign 2 (Higher O <sub>2</sub> /MEA)							
24	344974	88,0	-	5,59	1,64	4,52	13
144	332635	94,0	-	17,65	5,21	23,48	14
216	338570	77,0	-	24,82	8,37	34,2	18
312	342246	68,0	-	31,41	10,77	46,21	18
384	347595	60,0	-	35,77	12,4	63,43	8,6
Campaign 3 (Higher O <sub>2</sub> /stripping T 130°C)							
24	319000	63	-	3,4	2,5	<1	5,60
96	332000	87	-	9,9	3	4,6	7,20
192	320000	83	-	22	5,7	13	4,40
264	296000	65	-	29	6,6	17	2,60
360	300000	73	-	73	5,7	26	<1
Campaign 4 (Higher O <sub>2</sub> /NO <sub>x</sub> addition; mist formation)							
24	309000	120	<10	22	29	8,8	29
72	331000	140	<10	37	28	14	47
168	291000	110	<10	110,0	41	1600	30
240	396000	110	<10	130	43	2300	76
Campaign 5 (Baseline)							
24	311826	70,8	< 10	< 10	< 10	30,2	< 10
96	309066	69,5	< 10	< 10	< 10	37,1	< 10
192	314210	71,7	< 10	11,0	< 10	40,8	< 10
264	311359	61,2	< 10	13,6	< 10	43,1	< 10
360	282366	43,8	< 10	17,3	< 10	49,0	< 10
Campaign 6 (Higher O <sub>2</sub> /NO <sub>x</sub> addition)							
24	320184,1	101	< 10	< 10	< 10	30,5	10,4
72	320184,1	104	< 10	13,0	< 10	63,8	117,3
168	306501,1	115	< 10	77,6	13,6	161,7	203,0
240	306330	107	< 10	112,7	17,9	236,1	203,2

**Table C. 2: Karl-Fischer titration, FTIR and Phosphoric acid titration measurements for LAUNCH rig#2 campaigns**

Operational time hrs	Karl-Fischer	FTIR-Petten	FTIR-Delft				H <sub>3</sub> PO <sub>4</sub> Titration
	Water	CO <sub>2</sub>	MEA	Water	CO <sub>2</sub>	CO <sub>2</sub>	CO <sub>2</sub>
	%w/w	mol/l	wt%	wt%	wt%	mol/l	mol/l
Campaign 2 (Higher O <sub>2</sub> /MEA)							
24	65	1,65	34,82	58,96	6,35	1,64	1,58
144	65	1,68	33,97	59,38	6,67	1,71	1,60
216	64	1,71	34,62	58,58	6,76	1,73	1,52
312	64	1,80	35,41	57,51	7,04	1,81	1,57
384	67	2,08	36,00	55,85	8,12	2,08	1,93
Campaign 3 (Higher O <sub>2</sub> /stripping T 130°C)							
24	66	1,81	32,21	60,22	7,48	1,91	-
96	64	1,94	32,84	59,46	7,67	1,97	2,00
192	67	1,42	33,01	61,12	5,72	1,46	1,34
264	69	1,35	30,81	63,54	5,55	1,42	-
360	73	2,42	-	-	-	-	-
Campaign 4 (Higher O <sub>2</sub> /NO <sub>x</sub> addition; mist formation)							
24	68	1,59	32,91	60,68	6,32	1,61	1,51
72	66	1,96	33,69	58,32	7,91	2,02	-
168	70	1,55	31,57	62,19	6,17	1,57	-
240	57	2,60	32,21	59,5	8,29	2,11	-
Campaign 5 (Baseline)							
24	67,2	1,41	32,16	62,13	5,64	1,44	1,28
96	66,8	1,63	32,02	61,42	6,51	1,66	1,54
192	67,0	1,58	32,12	61,42	6,39	1,63	1,52
264	67,3	1,52	31,72	62,04	6,14	1,56	1,43
360	68,9	1,31	30,14	64,49	5,29	1,35	1,20
Campaign 6 (Higher O <sub>2</sub> /NO <sub>x</sub> addition)							
24	63,0	1,31	32,88	61,66	5,43	1,38	1,28
72	62,3	1,65	32,8	60,17	6,97	1,77	1,61
168	64,2	1,31	32,09	62,43	5,43	1,39	-
240	63,8	1,36	-	-	-	-	-

**Table C. 3: ICP-MS measurements for LAUNCH rig#2 campaigns**

Operational time hrs	ICP-MS*								
	Cr	Fe	Ni	Mn	Cu	Zn	Mo	Ba	Pb
	mg/kg	mg/kg	mg/kg	mg/kg	mg/kg	mg/kg	mg/kg	mg/kg	mg/kg
Campaign 2 (Higher O <sub>2</sub> /MEA)									
24	0,02	4,51	0,02	0,07	0,13	0,93	< 0,02	0,13	<0,01
144	0,13	3,70	0,22	0,07	< 0,1	1,52	0,05	0,17	<0,01
216	0,22	3,81	0,44	0,07	< 0,1	1,87	0,10	0,18	<0,01
312	0,32	4,41	0,78	0,08	< 0,1	2,28	0,18	0,20	<0,01
384	0,39	5,57	0,98	0,10	< 0,1	2,66	0,22	0,23	<0,01
Campaign 3 (Higher O <sub>2</sub> /stripping T 130°C)									
24	< 0,02	1,40	0,02	< 0,04	< 0,1	0,20	< 0,02	0,18	<0,01
96	0,17	3,50	0,19	0,04	< 0,1	0,76	0,04	0,18	<0,01
192	0,27	2,90	0,38	0,04	< 0,1	1,44	0,08	0,22	<0,01
264	0,40	5,30	0,51	0,06	< 0,1	2,07	0,10	0,27	<0,01
360	0,56	6,70	0,80	0,07	< 0,1	3,00	0,15	0,25	<0,01
Campaign 4 (Higher O <sub>2</sub> /NO <sub>x</sub> addition; mist formation)									
24	0,03	1,2	0,028	< 0,04	< 0,1	0,28	< 0,02	0,03	<0,01
72	0,056	1,7	0,056	< 0,04	< 0,1	0,52	< 0,02	0,05	<0,01
168	0,15	1,6	0,15	< 0,04	< 0,1	1,12	0,02	0,08	<0,01
240	0,24	2,4	0,24	0,05	< 0,1	1,97	0,04	0,12	<0,01
Campaign 5 (Baseline)									
24	< 0,02	0,74	< 0,02	< 0,04	< 0,1	0,25	< 0,02	0,03	<0,01
96	0,09	1,18	0,05	< 0,04	< 0,1	0,69	< 0,02	0,04	<0,01
192	0,12	1,20	0,07	< 0,04	< 0,1	1,05	< 0,02	0,05	<0,01
264	0,16	1,40	0,11	< 0,04	< 0,1	1,62	< 0,02	0,05	<0,01
360	0,21	1,24	0,25	< 0,04	< 0,1	2,17	0,05	0,04	<0,01
Campaign 6 (Higher O <sub>2</sub> /NO <sub>x</sub> addition)									
24	0,023	0,847	< 0,02	< 0,04	< 0,1	0,32	< 0,02	0,02	<0,01
72	0,09	1,30	0,04	< 0,04	< 0,1	0,66	< 0,02	0,04	<0,01
168	0,16	1,16	0,12	< 0,04	< 0,1	1,47	< 0,02	0,03	<0,01
240	0,21	1,01	0,17	< 0,04	< 0,1	2,14	0,02	0,04	<0,01

**Table C. 4: LC-MS measurements for LAUNCH rig#2 campaigns**

Operational time hrs	LC-MS (SINTEF)													
	MEA g/L	MEA-Urea mg/L	HEHEAA mg/L	HEEDA mg/L	2-oxazoline mg/L	HEI mg/L	HEF mg/L	HEPO mg/L	HeGly mg/L	HEA mg/L	BHEOX mg/L	HEIA mg/L	OZD mg/L	Nitroso-HeGly mg/L
Campaign 2 (Higher O <sub>2</sub> /MEA)														
24	377	105	198	< 1	n.d.*	562	734	69,0	199	21,9	25,4	0,5	9,7	< 0,50
144	368	1546	217	< 1	n.d.	660	774	1597	487	77,1	30,6	9,4	35,8	< 0,50
216	367	2190	266	< 1	n.d.	1075	1162	3219	792	120	45,3	20,5	43,9	< 0,50
312	378	2806	254	< 1	n.d.	1058	1171	5350	886	146	49,5	42,1	55,1	< 0,50
384	393	3589	193	< 1	n.d.	291	421	8021	893	160	19,3	75,1	67,8	< 0,50
Campaign 3 (Higher O <sub>2</sub> /stripping T 130°C)														
24	355	123	127	< 1	n.d.	189	321	46,0	95,1	11,2	21,4	0,2	19,5	< 0,50
96	373	2360	113	< 1	n.d.	219	362	2766	198	26,3	32,9	27,9	66,3	< 0,50
192	355	2816	80,3	1,5	n.d.	218	436	7732	218	43,5	15,5	164	50,4	< 0,50
264	325	3090	53,0	5,7	n.d.	130	437	11403	222	55,3	12,0	362	64,7	< 0,50
360	347	3574	38,0	2342	n.d.	39	214	8740	211	75,0	< 10	899	85,2	< 0,50
Campaign 4 (Higher O <sub>2</sub> /NO <sub>x</sub> addition; mist formation)														
24	353	78,4	166	< 1	n.d.	422	703	54,0	215	17,5	19,4	2,1	10,5	< 0,50
72	362	665	187	< 1	n.d.	1027	1356	431	410	39,3	98,0	7,2	34,5	0,5
168	344	2286	149	< 1	n.d.	281	492	2372	651	219	< 10	31,2	48,3	18,4
240	355	2586	130	< 1	n.d.	121	313	3490	653	258	11,4	46,7	68,7	20,8
Campaign 5 (Baseline)														
24	337	50,1	106	< 1	n.d.	241	378	22,5	84	14,0	< 10	0,2	7,1	< 0,50
96	366	987	94,7	< 1	n.d.	124	238	567	191	17,2	< 10	3,3	31,0	< 0,50



192	348	1635	101	< 1	n.d.	230	404	1720	232	25,0	< 10	14,7	36,6	< 0,50
264	341	2001	81,3	< 1	n.d.	188	337	2918	236	30,4	< 10	34,0	42,8	< 0,50
360	320	2086	49,9	< 1	n.d.	104	281	4432	229	31,6	< 10	71,6	42,3	< 0,50
Campaign 6 (Higher O <sub>2</sub> /NO <sub>x</sub> addition)														
24	349	31,4	118	< 1		351	462	22,0	63,0	12,5	< 10	0,3	5,7	< 0,50
72	358	593	116	< 1		168	288	303	240	39,0	< 10	1,9	20,0	0,8
168	336	1873	131	< 1		239	400	1855	579	217	< 10	20,8	38,1	10,3
240	336	2489	158	< 1		197	493	3250	623	328	< 10	43,3	37,8	19,5

\*n.d.: not detected

**Table C. 5: IC measurements for TERC campaigns**

Operational time hrs	IC										
	Glycolic Acid	3-OH Propionic Acid	Lactic Acid	Formic Acid	3-OH Butyric Acid	Acetic Acid	Propionic Acid	Isobutyric Acid	Butyric Acid	Glyoxylic Acid	
	mg/kg	mg/kg	mg/kg	mg/kg	mg/kg	mg/kg	mg/kg	mg/kg	mg/kg	mg/kg	
Campaign 2 (Higher O <sub>2</sub> /MEA)											
0	7,8	< 5	< 5	50	< 5	< 5	< 0,5	< 0,5	< 0,5	< 0,5	
29	6,2	< 5	< 5	50	< 5	< 5	< 0,5	< 0,5	< 0,5	< 0,5	
63	7,6	< 5	< 5	50	< 5	< 5	< 0,5	< 0,5	< 0,5	< 0,5	
88	8,6	< 5	< 5	50	< 5	< 5	< 0,5	< 0,5	< 0,5	< 0,5	
118	7,6	< 5	< 5	50	< 5	< 5	< 0,5	< 0,5	< 0,5	< 0,5	
160	7,8	< 5	< 5	50	< 5	< 5	< 0,5	< 0,5	< 0,5	< 0,5	
Campaign 3 (Higher O <sub>2</sub> /stripping T 128°C)											
0	15,4	< 5	< 5	50	< 5	< 5	< 0,5	< 0,5	< 0,5	< 0,5	
25	31,7	< 5	< 5	50	< 5	< 5	< 0,5	< 0,5	< 0,5	< 0,5	



65	27,5	< 5	< 5	50	< 5	< 5	< 0,5	< 0,5	< 0,5	< 0,5
139	41,0	< 5	10,1	50	< 5	6,5	< 0,5	< 0,5	< 0,5	< 0,5
161	42,4	< 5	51,4	50	< 5	8,3	< 0,5	< 0,5	< 0,5	< 0,5
Campaign 4 (Higher O <sub>2</sub> /NO <sub>x</sub> addition)										
0	7,2	< 5	< 5	50	< 5	7,3	< 0,5	< 0,5	< 0,5	< 0,5
35.5	22,7	< 5	< 5	69	< 5	12,5	< 0,5	< 0,5	< 0,5	< 0,5
83.5	36,5	< 5	< 5	89	< 5	14,5	< 0,5	< 0,5	< 0,5	< 0,5
108.5	36,4	< 5	< 5	93	< 5	19,1	< 0,5	< 0,5	< 0,5	< 0,5
152	47,0	< 5	< 5	113	< 5	23,7	< 0,5	< 0,5	< 0,5	< 0,5
Campaign 5 (Baseline)										
20	10,3	< 5	< 5	50	< 5	10,3	< 0,5	< 0,5	< 0,5	< 0,5
86	15,8	< 5	< 5	97	< 5	19,0	< 0,5	< 0,5	< 0,5	< 0,5
118	18,4	< 5	< 5	73	< 5	18,0	< 0,5	< 0,5	< 0,5	< 0,5
162	25,8	< 5	< 5	90	< 5	19,3	< 0,5	< 0,5	< 0,5	< 0,5

**Table C. 6: Colorimetric measurements for Fe in TERC campaigns**

Campaign 2 (Higher O <sub>2</sub> /MEA)		Campaign 3 (Higher O <sub>2</sub> /stripping T 128°C)		Campaign 4 (Higher O <sub>2</sub> /NO <sub>x</sub> addition)		Campaign 5 (Baseline)	
Operational time	Fe	Operational time	Fe	Operational time	Fe	Operational time	Fe
hrs	mg/L	hrs	mg/kg	hrs	mg/kg	hrs	mg/kg
0	0	0	0,02	0	0,02	0	0,03
4	0,52	17	0,41	14	0,68	20	0,57
29	1,23	25	0,45	35,5	0,57	86	0,64
51	1,45	41	0,4	57,5	0,73	118	0,74
59	1,5	65	0,37	83,5	0,8	162	0,76
63	1,51	139	0,38	108,5	0,73		
88	1,74	167	0,41	152	0,83		
95	1,84	186	0,39				
111	2	192	0,43				
118	2,08						
135	2,19						
160	2,36						
165	2,4						
191	2,9						
214	2,89						
231	2,86						
256	2,97						
261	3						
279	3,09						
284	3,04						
286	3,08						
308	3,24						
328	3,43						
350	3,95						

**Table C. 7: IC measurements for TERC campaigns**

Operational time hrs	LC-MS (SINTEF)												
	MEA	HEI	HEF	HEPO	HeGly	HEA	BHEOX	HEIA	OZD	MEA-Urea	HEHEAA	HEEDA	Nitroso-HeGly
	mg/kg	mg/kg	mg/kg	mg/kg	mg/kg	mg/kg	mg/kg	mg/kg	mg/kg	mg/kg	mg/kg	mg/kg	mg/kg
	Campaign 2 (Higher O <sub>2</sub> /MEA)												
0	373	1,86	7,75	17,9	48,0	2,35	< 1	0,20	< 0,1	12,1	4,41	< 1	< 1
29	447	27,0	83,6	193	182	11,0	5,66	0,54	9,97	483	94,8	< 1	< 1
63	399	6,32	43,8	423	216	13,3	2,01	1,47	12,1	860	49,1	1,47	< 1
88	396	7,33	42,3	659	252	19,0	2,20	2,75	13,5	1120	53,8	2,66	< 1
118	395	16,0	74,8	1010	305	24,0	3,57	4,58	16,4	1400	67,1	1,19	< 1
160	394	15,1	73,4	1510	341	32,8	3,58	8,62	18,6	1730	66,0	6,60	< 1
	Campaign 3 (Higher O <sub>2</sub> /stripping T 128°C)												
0	324	0,60	4,07	0,60	25,1	1,69	< 1	< 0,1	< 0,1	0,298	2,78	< 1	< 1
25	344	42,4	134	138	341	19,8	1,45	1,16	1,83	241	79,6	< 1	< 1
65	338	57,9	154	348	502	24,9	1,45	3,09	1,84	395	91,0	< 1	< 1
139	331	33,7	121	839	757	33,1	1,74	5,02	1,93	567	82,0	< 1	< 1
161	327	83,1	228	962	781	37,6	2,52	5,81	1,84	599	102	< 1	< 1
	Campaign 4 (Higher O <sub>2</sub> /NO <sub>x</sub> addition)												
0	< 1	6,4	1,8	9,2	1,8	< 1	< 1	< 1	2,4	2,6	< 1	< 0,1	< 1
35.5	59	115	94	203,9	11	2	< 1	7,2	258	103,3	< 1	< 0,1	59
83.5	33	112	514	470,9	51,4	4,3	4,4	15,1	905	101,2	< 1	0,56	33
108.5	49	131	762	541,1	58,8	5,6	6,7	20,4	1055	121,6	< 1	0,79	49
152	14	96	1379	735,6	92	5,2	13,4	28,4	1600	98,6	2,9	5,1	14
	Campaign 5 (Baseline)												
20	4.1	32,7	83,6	96,4	5,1	< 1	< 1	8,7	242	20,1	3,6	< 0,1	4,1



86	3.5	26,1	329	164	13,1	< 1	1,8	22,7	990	22	52,6	< 0,1	3,5
118	3.1	22,6	384	187	9,6	2,6	3,3	28,8	1246	21,9	131,5	< 0,1	3,1
162	2.8	22,1	546	210,8	15,6	3	7,7	33,4	1642	24	252	< 0,1	2,8